PARAMETRIC SCALING LAWS. PART I. AN ANALYTICAL MODEL FOR PREDICTING THE SATURATION LIMITS OF A PARAMETRIC ARRAY

F. H. Fenlon

Westinghouse Electric Corporation

Prepared for:

Office of Naval Research
Defense Contract Administration Services District
Advanced Research Projects Agency

22 August 1974

PARAMETRIC SCALING LAWS

F. H. Fenlon

Final Report, Part I - A003
"An Analytical Model for Predicting the Saturation Limits of a Parametric Array"

ARPA Order Number:	2655/11-30-73
Program Code Number:	4E20
Effective Date of Contract:	February 1, 1974
Contract Expiration Date:	July 31, 1974
Amount of Contract:	$29,591
Contract Number:	N00014-74-C-0214
Principle Investigator:	F H. Fenlon (412) 256-3676
Scientific Officer:	R. Obrochta

Sponsored by Advanced Research Projects Agency
ARPA Order No. 2655/11-30-73

This research was supported by the Advanced Research Projects Agency of the Department of Defense and was monitored by ONR under Contract No. N00014-74-C-0214.

August 22, 1974

WESTINGHOUSE RESEARCH LABORATORIES PITTSBURGH, PA. 15235

Unclassified

SECURITY CLASSIFICATION OF THIS PAGE *(When Data Entered)*

REPORT DOCUMENTATION PAGE

READ INSTRUCTIONS BEFORE COMPLETING FORM

1 REPORT NUMBER

2 GOVT ACCESSION NO.

3 RECIPIENT'S CATALOG NUMBER

4 TITLE *(and Subtitle)*
PARAMETRIC SCALING LAWS - Part I - An Analytical Model for Predicting the Saturation Limits of a Parametric Array

5 TYPE OF REPORT & PERIOD COVERED
Final Report - (Part I)
1 Feb. 1974 to 31 July 1974

6 PERFORMING ORG. REPORT NUMBER
72-9M7-NONLN-R2

7 AUTHOR(s)
F. H. Fenlon

8 CONTRACT OR GRANT NUMBER(s)
N00014-74-C-0214

9 PERFORMING ORGANIZATION NAME AND ADDRESS
Westinghouse Electric Corporation
Research & Development Center
Beulah Road, Pittsburgh, PA [illegible]

10 PROGRAM ELEMENT, PROJECT, TASK AREA & WORK UNIT NUMBERS
ARPA Order No. 2655/11-30-73
Program Code No. 4E20

11 CONTROLLING OFFICE NAME AND ADDRESS
Procuring Contracting Officer
Office of Naval Research
Department of the Navy
Arlington, VA 22217

12 REPORT DATE
August 22, 1974

13 NUMBER OF PAGES
66

14 MONITORING AGENCY NAME & ADDRES *(if different from Controlling Office)*
Commander, Defense Contract Administration
Sercices District
1610-S Federal Building, 1000 Liberty Ave.
Pittsburgh, PA 15222

15 SECURITY CLASS. *(of this report)*
Unclassified

15a DECLASSIFICATION/DOWNGRADING SCHEDULE

16 DISTRIBUTION STATEMENT *(of this Report)*

17 DISTRIBUTION STATEMENT *(of the abstract entered in Block 20, if different from Report)*
NA

18 SUPPLEMENTARY NOTES

19 KEY WORDS *(Continue on reverse side if necessary and identify by block number)*
Nonlinear, saturation, sonar.

20 ABSTRACT *(Continue on reverse side if necessary and identify by block number)*

Following a review of the approximate models previously used to provide parametric scaling laws, an exact solution for the asymptotic far-field pressure of a parametric array is derived from the plane wave form of Burgers' equation. The influence of spherical spreading losses is then included by matching the solution at low primary wave amplitudes with a spherical wave solution obtained by the method of successive approximation. From the matched asymptotic solution, the referred pressure of the difference-

DD FORM 1 JAN 73 1473 EDITION OF 1 NOV 65 IS OBSOLETE

Unclassified

SECURITY CLASSIFICATION OF THIS PAGE *(When Data Entered)*

20. cont'd.

frequency signal at one meter from the source (i.e., the equivalent difference-frequency source level) is derived as a universal function of scaled primary wave amplitudes, frequencies, source dimensions, and physical constants of the medium. With the aid, this function, which defines the saturation limit of a parametric array, the maximum conversion efficiency can be evaluated for a particular set of input parameters. The amplitude dependence of the directivity function and directivity index for "spreading loss limited" parametric arrays can also be determined. Scaled performance characteristics obtained from the model are shown to be in good agreement with data published in the literature over quite a wide range of scaled primary wave source parameters.

PARAMETRIC SCALING LAWS

Part I: An Analytical Model for Predicting the Saturation Limits of a Parametric Array

by

F. H. Fenlon

SUMMARY

Following a review of the approximate models previously used to provide parametric scaling laws, an exact solution for the asymptotic far-field pressure of a parametric array is derived from the plane wave form of Burgers' equation. The influence of spherical spreading losses is then included by matching the solution at low primary wave amplitudes with a spherical wave solution obtained by the method of successive approximation. From the matched asymptotic solution, the referred pressure of the difference-frequency signal at one meter from the source (i.e., the equivalent difference-frequency source level) is derived as a universal function of scaled primary wave amplitudes, frequencies, source dimensions, and physical constants of the medium. With the aid, this function, which defines the saturation limit for a parametric array, the maximum conversion efficiency can be evaluated for a particular set of input parameters. The amplitude dependence of the directivity function and directivity index for "spreading loss limited" parametric arrays can also be determined. Scaled performance characteristics obtained from the model are shown to be in good agreement with data published in the literature over quite a wide range of scaled primary wave source parameters.

TABLE OF CONTENTS

LIST OF SYMBOLS

ρ_o	density of the medium
c_o	small signal speed of sound
$\beta = 1 + (B/2A)$	nonlinear parameter for liquids
$= \frac{1}{2}(1 + \frac{C_p}{C_v})$	in gases
A, B	first and second-order coefficients in the equation of state
C_p, C_v	specific heats at constant pressure and constant volume
$r, r_o, r_o' = r_o(\omega_o/\omega_-)$	range, Rayleigh distance, and end-fire truncation distance
$t, t' = t-(r-r_o/c_o)$	time and retarded time
$f, f_i (i=1,2)$	frequency and primary wave frequencies
$f_o = \frac{1}{2}(f_1+f_2)$	mean primary wave frequency
$f_- = f_1-f_2$	difference-frequency
$\omega = 2\pi f, \omega_i (i=1,2)$	angular frequency and angular primary wave frequencies
ω_o, ω_-	mean angular primary wave frequency and angular difference frequency
$\omega_{nm} = n\omega_1 \pm m\omega_2$	angular combination frequencies
$k = \omega/c_o, k_i (i=1,2)$	wave number and primary wave numbers
k_o, k_-	mean primary wave number and difference frequency wave number
ϕ_i $(i=1,2)$	primary wave phases
$\phi_{nm} = n\phi_1 \pm m\phi_2$	combination phases
p'	excess pressure
p_{oi}, $(i=1,2)$	primary wave amplitudes at the source

$p_o = (p_{o1}+p_{o2})$	peak primary wave amplitude at the source
$\bar{p}_{oi} = p_{oi}/\sqrt{2}, (i=1,2)$	rms primary wave amplitudes at the source
$\bar{p}_o = \sqrt{(\bar{p}_{o1})^2+(\bar{p}_{o2})^2}$	total rms primary wave amplitude at the source
$P = (r/r_o)^{\ell}(p'/p_o)$	normalized field pressure
$\ell = 0,\ 1/2,\ 1$	for plane, cylindrical or spherical waves
$\breve{p}_{\omega}(r)$	Fourier transform of $P(r,t')$
$p'_{-}(r)$	far-field difference frequency spectral amplitude
$p_{1,2} = p_{o1} = p_{o2}$	for equal primary wave amplitudes at the source
$T_N,\ T_F$	near and far-field finite-amplitude absorption tapers
$\delta = \alpha/\omega^2$	nondispersive thermo viscous attenuation parameter
α	attenuation coefficient
α_o	mean primary wave attenuation coefficient
$\alpha_i (i=1,2)$	primary wave attenuation coefficients
α_-	difference-frequency attenuation coefficient
$\alpha_T = (\alpha_1+\alpha_2-\alpha_-)$	total attenuation coefficient
α_{nm}	combination frequency attenuation coefficients
$\alpha_T r_o \simeq 2\alpha_o r_o$ if $\alpha_1 \simeq \alpha_2 >> \alpha_-$	near field primary wave absorption loss
σ	distortion parameter
$\sigma'_o = \beta p_o r_o/\rho_o c_o^3$	
$\sigma_o = \sigma'_o \omega_o$	mean primary wave distortion parameter
$\sigma_i = \sigma_o(p_{oi}/p_o), (i=1,2)$	primary wave distortion parameters
$\sigma_{1,2} = \sigma_o(p_{o1}p_{o2}/p_o^2)$	
$\Lambda_o = \sigma'_o/\delta r_o$	
$\chi'_o = \Gamma_o = (\Lambda_o/\omega_o)$	combined primary wave acoustic Reynolds number
$\chi'_i = \Gamma_i = (\Lambda_o/\omega_i)(p_{oi}/p_o), (i=1,2)$	primary wave Reynolds numbers
$\chi''_o = \sigma_o E_1(\alpha_T r_o)$	

$\chi_i'' = \sigma_i E_1(\alpha_T r_o), (i=1,2)$

$\chi_o = \sigma_o \Delta$

$\chi_i = \sigma_i \Delta, \ (i=1,2)$

$\Delta = E_1(\alpha_T r_o)\exp(\alpha_T r_o)$

$\Delta' = E_1(\alpha_T r_o')\exp(\alpha_T r_o')$

$n = 1 + \{\frac{\log_{10}(\Delta/\Delta')}{\log_{10}(\omega_o/\omega_-)}\}$ parametric frequency response index

$D_i(\theta,\phi), \ (i=1,2)$ normalized primary wave directivity functions

θ_- virtual end-fire-array half power beamwidth

$\theta_-^{\infty} = 4\sqrt{\alpha_1/k_-}$ virtual end-fire-array half power beamwidth for an "absorption-limited" parametric array

θ_o primary wave product pattern half power beamwidth

$\psi(\zeta,t) = \exp\{(\Lambda_o/2)\int_o^t P(\zeta,t')dt'\}$

$SL_o = 20 \log_{10}(\bar{p}_o r_o)$ combined rms primary wave source level at 1 m

$SL_i = 20 \log_{10}(\bar{p}_{oi} r_o), (i=1,2)$ rms primary wave source level at 1 m

$SL_{1,2} = SL_1 = SL_2$ denotes equal rms primary wave source levels

$SL_- = 20 \log_{10}\{p_-'(r)\cdot r \exp(\alpha_- r)\}$ equivalent rms difference-frequency source level at 1 m

$SL_o^* = SL_o + 20 \log_{10} f_o, (f_o \text{ in kHz})$ scaled combined primary wave source level

$SL_i^* = SL_i + 20 \log_{10} f_o, (i=1,2)$ scaled primary wave source levels

$SL_-^* = SL_- + 20 \log_{10} f_o$ scaled difference-frequency source level

$SL_o^{**} = SL_o^* + 20 \log_{10}\Delta$ double scaled combined primary wave source level

$SL_i^{**} = SL_i^* + 20 \log_{10}\Delta, (i=1,2)$ double scaled primary wave source levels

$SL_-^{**} = SL_-^* + 20 \log_{10}\Delta - 20 \log(f_-/f_o)^n$ source level double scaled difference-frequency source level

$$E_1(z) = \int_z^\infty \frac{e^{-x}}{x}\,dx \qquad \text{Exponential integral}$$

$$\to -\ln(z) - \sum_{m=1}^{\infty} \frac{(-1)^m z^m}{m\,m!} - 0.57721, \quad |z| \ll 1;\ |\arg z| < \pi$$

$$\to \left(\frac{e^{-z}}{z}\right)\left(1 - \frac{1}{z} + \frac{2}{z^2}\right) \quad , \quad |z| \gg 1;\ |\arg z| < \frac{3\pi}{2}$$

$H_o(z) \to (2/\pi)z, \quad z \ll 1 \qquad$ Struve Function

$$\to (2/\pi)\left(\frac{1}{z} - \frac{1}{z^3} + \ldots\right), \quad z \gg 1;\ |\arg z| < \pi$$

$Y_o(z) \to (2/\pi)\ln(z), \quad z \ll 1 \qquad$ Neumann Function

$$\to \sqrt{(2/\pi z)}\ \{\sin(z - \tfrac{\pi}{4})\}, \quad z \gg 1;\ |\arg z| < \pi$$

$I_n(z)$ Bessel function of imaginary argument

FIGURE CAPTIONS

Fig. 1 Schematic representation of a parametric source.

Fig. 2 Comparison of unsaturated parametric array models.

X Mellen, Moffett[1,2]

\- Fenlon[3]

● Berktay, Leahy[4]

Fig. 3 Dependence of the parametric frequency response index n on $\alpha_T r_o$ and f_o/f_-.

Fig. 4 Universal 'input-output' characteristic of a parametric array for equal drive amplitudes.

Fig. 5 Amplitude dependence of the far-field difference-frequency beam pattern for a 'spreading-loss limited' parametric array.

Fig. 6a Scaled parametric 'input-output' characteristics in water, for equal drive amplitudes, with $\alpha_T r_o = 10^{-5}$ dB.

Fig. 6b Conversion efficiency vs scaled source level characteristics in water, for equal drive amplitudes, with $\alpha_T r_o = 10^{-5}$ dB.

Fig. 7a Scaled parametric 'input-output' characteristics in water, for equal drive amplitudes, with $\alpha_T r_o = 10^{-1}$ dB.

Fig. 7b Conversion efficiency vs scaled source level characteristics in water, for equal drive amplitudes, with $\alpha_T r_o = 10^{-1}$ dB.

Fig. 8a Scaled parametric 'input-output' characteristics in water, for equal drive amplitudes, with $\alpha_T r_o = 10^{2}$ dB.

Fig. 8b Conversion efficiency vs scaled source level characteristics in water, for equal drive amplitudes, with $\alpha_T r_o = 10^2$ dB.

Fig. 9 Comparison of saturated and partially saturated parametric array models.

Fig. 10a Comparison of scaled universal parametric 'input-output' characteristic in water with experimental data, for equal drive amplitudes.

- ● NUSC[34], f_o = 175 kHz; f_- = 12 kHz, 3 kHz
- Δ NUSC[34], f_o = 250 kHz; f_- = 12 kHz, 6 kHz
- ▯ NUSC[34], f_o = 720 kHz; f_- = 100 kHz, 50 kHz, 25 kHz, 12.5 kHz
- O NUSC[35], f_o = 330 kHz; f_- = 60 kHz, 30 kHz, 15 kHz, 6 kHz
- Θ NUSC[36], f_o = 65 kHz, f_- = 3.5 kHz
- ◇ Muir, Willette[37], f_o = 450 kHz; f_- = 64 kHz
- ◐ Eller[38], f_o = 1435 kHz; f_- = 50 kHz

Fig. 10b Comparison of a scaled universal conversion efficiency characteristic in water with experimental data, for equal drive amplitudes.

- ● NUSC[34], f_o = 175 kHz; f_- = 12 kHz, 3 kHz
- Δ NUSC[34], f_o = 250 kHz; f_- = 12 kHz, 6 kHz
- □ NUSC[34], f_o = 720 kHz; f_- = 100 kHz, 50 kHz, 25 kHz, 12.5 kHz
- O NUSC[35], f_o = 330 kHz; f_- = 60 kHz, 30 kHz, 15 kHz, 6 kHz
- Θ NUSC[36], f_o = 65 kHz; f_- = 3.5 kHz
- ◇ Muir, Willette[37], f_o = 450 kHz; f_- = 64 kHz
- ◐ Eller[38], f_o = 1435 kHz; f_o = 50 kHz

TABLE CAPTIONS

INTRODUCTION

In order to facilitate the design of parametric arrays, different investigators[1-5] guided by experimental observation have constructed performance characteristics from simple approximate solutions of the second-order nonlinear wave equation.[6] These solutions comprise (1) Westervelt's[7] far-field approximation for the difference-frequency signal generated by nonlinear interaction of infinitely plane unsaturated primary waves of finite amplitude (i.e., waves whose peak amplitudes are below their respective shock thresholds), subject only to viscous absorption, and (2) the corresponding approximation for unsaturated spherical primary waves derived by Cary[8] and the author.[8,9] As shown in Fig. 1, the primary wave fields of a finite-amplitude source of area S_o, embedded in an infinite rigid baffle, operating simultaneously at angular frequencies ω_1 and ω_2 can be treated as plane collimated waves within a distance from the source $r_o = S_o/\lambda_o$ (described as the "collimation distance" or "Rayleigh distance") where λ_o is the wavelength of the mean primary wave frequency. At distances greater than r_o the primary fields can be represented as spherically spreading waves. If the near field primary wave absorption loss $\alpha_T r_o$ is large enough to ensure that the primary waves are sufficiently absorbed within r_o to the extent that no further nonlinear interaction occurs beyond this range, the parametric array is said to be "absorption limited," and Westervelt's solution[7] can be used in this instance to determine the pre-shock asymptotic far-field form of the difference-frequency signal.

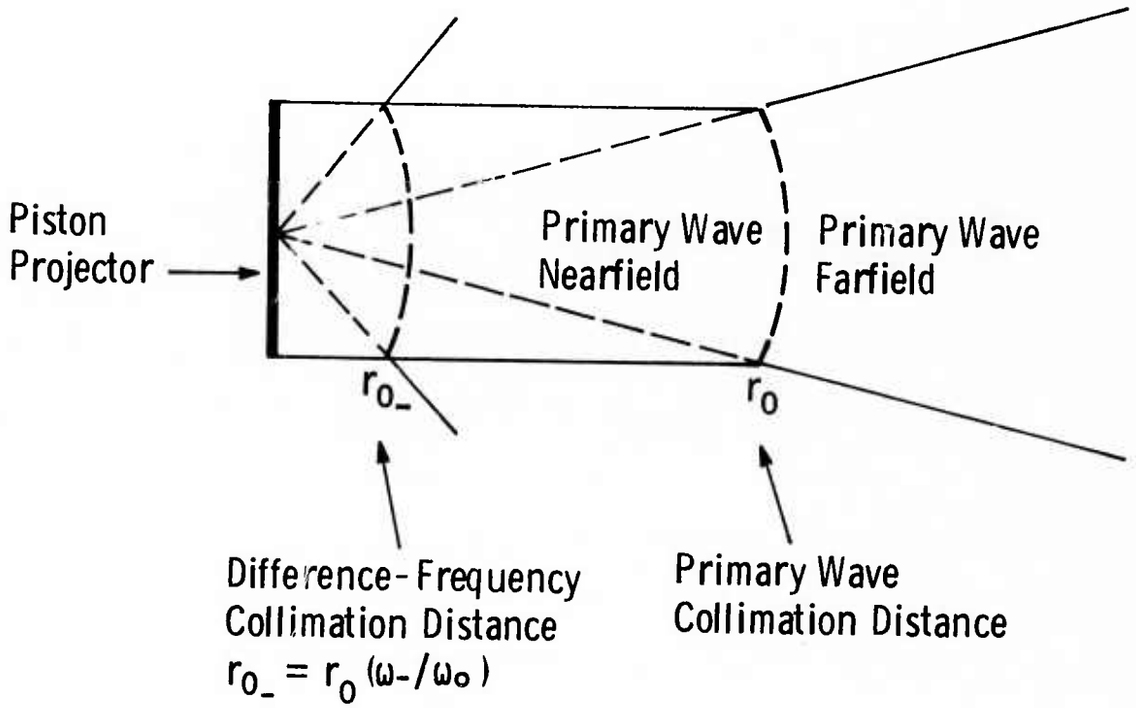
Piston
Projector
Primary Wave
Nearfield
Primary Wave
Farfield
r_{0-}
r_0
Difference-Frequency
Collimation Distance
$r_{0-} = r_0 (\omega_- / \omega_o)$
Primary Wave
Collimation Distance

Fig. 1

On the other hand, if $\alpha_T r_o$ is very small, the primary wave interaction takes place primarily beyond r_o and is limited essentially by spreading losses, so that in this instance the spherical wave solutions[8,9] can be used to define the pre-shock difference frequency pressure in the far-field of the parametric array. Within r_o a virtual-end-fire array is formed whose half-power beamwidth $\theta_-(r)$ at pre-shock primary wave amplitudes decreases with range as $\sqrt{\lambda_-/r}$. If the array is "absorption limited" its final length is entirely determined by the primary wave absorption coefficient α_T, so that the limiting far-field beamwidth $\theta_-^\infty = \sqrt{\lambda_- \alpha_T} \simeq 4\sqrt{\alpha_T/2k_-}$.

Alternatively, if nonlinear interaction also takes place beyond r_o, the end-fire array length is curtailed both by viscous absorption and by spreading losses. In this instance, as r increases, the half-power beamwidth $\theta_-(r)$ asymptotically approaches that of the primary wave product beam pattern θ_o formed beyond r_o, where $\theta_o \sim \pi/k_o a$ for a circular piston source of radius a with $k_o a > 1$, operating at pre-shock primary wave amplitudes. Eventually, $\theta_-(r)$ equals θ_o at a range $r_o' = r_o(\omega_o/\omega_-)$.

Likewise as shown by the author[3] it follows that if $\alpha_T r_o' >> 1$, the parametric array is absorption limited so that the far-field half-power beamwidth is θ_-^∞ at pre-shock primary wave amplitudes. Alternatively, under the same conditions if $\alpha_T r_o' << 1$ then θ_o will be the far-field beamwidth. Thus, by identifying $\alpha_T r_o'$ as the key parameter which determines whether a parame. ic array is "absorption limited" or "spreading loss limited", Mellen and Moffett[1,2] combined the simple plane and spherical

wave solutions[7-9] to obtain an approximate asymptotic far-field solution for all values of $\alpha_T r'_o$. This solution can be expressed as,

$$p'_-(r)/p_o = -(\sigma_{1,2}/2)\{(\omega_-/\omega_o)^2\int_o^{r'_o} T_N^2(r')e^{-\alpha_T r'}\frac{dr'}{r_o} - j(\omega_-/\omega_o)\int_{r'_o}^{\infty} T_F^2(r')e^{-\alpha_T r'}\frac{dr'}{r'}\}(\frac{r_o}{r})e^{-\alpha_- r}, \quad (1)$$

where all variables are defined in the list of symbols and p_- is normalized with respect to the peak amplitude at the source p_o, rather than to either of the individual primary wave amplitudes, as in the Mellen and Moffett[1,2] model (where the latter are assumed to be equal).

If the amplitude taper functions T_N and T_F, which account symbolically for finite-amplitude absorption of the primary waves, are set equal to unity, the terms in Eq. 1 can be combined and integrated in various ways giving the unsaturated solutions shown in Table 1a. Inspection of Fig. 2 also shows that these unsaturated solutions are in good agreement over a wide range of $\alpha_T r'_o$. Mellen and Moffett's model[1,2] goes beyond the unsaturated case however, by providing an explicit expression for the amplitude taper functions T_N and T_F, which are assumed to be of equal weight. This expression, which is of the form, $T_N = T_F = 1/\sqrt{1+(\sigma/2)^2}$, was obtained by empirical observation of the extent to which the peak amplitude of a monofrequency finite-amplitude wave is reduced due to phase advancement; the "distortion parameter" σ being determined by the extend to which the peak of the waveform advances in an inviscid fluid,

$$[\text{i.e., } \sigma \approx \sigma_o\int_o^{r_o}\frac{dr'}{r_o} - j\sigma_o\int_{r_o}^{r}\frac{dr'}{r'} \approx \sigma_o\int_o^{r}\frac{d(r'/r_o)}{\sqrt{1+(r'/r_o)^2}} = \sigma_o \sinh^{-1}(r/r_o)].$$

Substitution of such a taper function in Eq. 1 however, assumes that the primary fields can be treated as independent monofrequency waves losing energy only through transfer to self-generated second harmonics.

TABLE 1a

$|p'_-(r)/p_o| \rightarrow (\omega_-/\omega_o)(\sigma_{1,2}/2)(\Delta')(r_o/r)e^{-\alpha_- r}$; $(\sigma_o/2)(\Delta) << 1$; $\alpha_T r_o \simeq 2\alpha_o r_o$

Model	Δ'	$\lim(\Delta')$, $\alpha_T r'_o >> 1$	$\lim(\Delta')$, $\alpha_T r'_o << 1$
Mellen, Moffett[1,2]	$\int_o^\infty \frac{\exp(-X)dX}{\sqrt{(\alpha_T r'_o)^2 + X^2}} = (\pi/2)[H_o(\alpha_T r'_o) - Y_o(\alpha_T r'_o)]$	$(\omega_-/\omega_o)(1/\alpha_T r_o)$	$\ln(\alpha_T r'_o)$
Fenlon[3]	$\int_o^\infty \frac{\exp(-X)dX}{\alpha_T r'_o + X} = E_1(\alpha_T r'_o)\exp(\alpha_T r'_o)$	$(\omega_-/\omega_o)(1/\alpha_T r_o)$	$E_1(\alpha_T r'_o)$
Berktay, Leahy[4]	$\sqrt{(1-e^{-\alpha_T r'_o})^2 (1/\alpha_T r'_o)^2 + [E_1(\alpha_T r'_o)]^2}$	$(\omega_-/\omega_o)(1/\alpha_T r_o)$	$E_1(\alpha_T r'_o)$
Bartram[5]	$(1/\alpha_T r'_o)$	$(\omega_-/\omega_o)(1/\alpha_T r_o)$	-

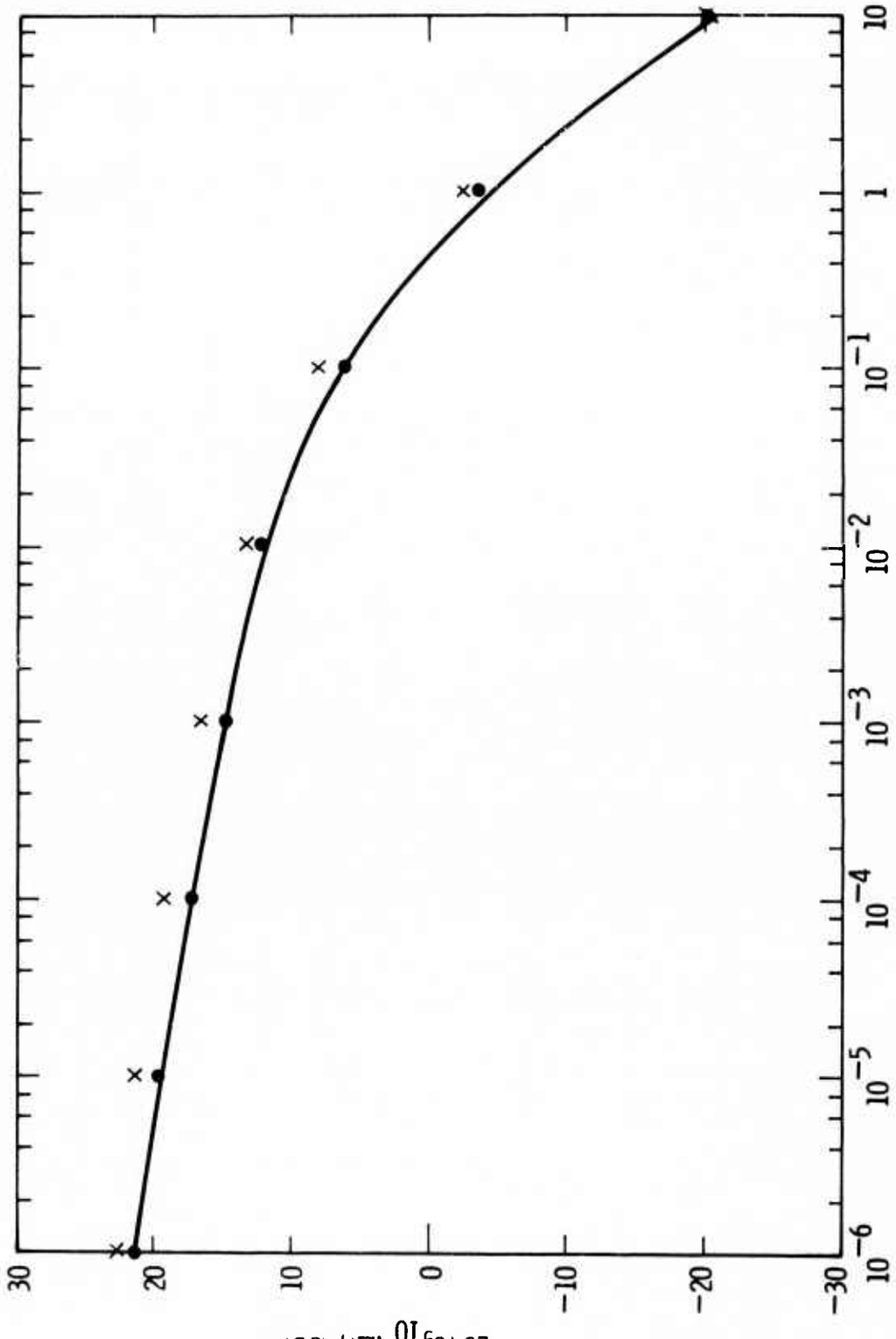
30
20
10
0
−10
−20
−30
$20 \log_{10} (\Delta')$, (dB)
10^{-6}
10^{-5}
10^{-4}
10^{-3}
10^{-2}
10^{-1}
1
10
$\alpha_T r_o'$ (Nepers)

Fig. 2

Thus, in making this assumption the additional loss of energy transferred to higher self-generated harmonics is neglected, in addition to degenerative coupling of the type discussed by Tjotta,[10] Hobaek and Vistrheim,[11] due to interaction of the sum frequency component and the primary waves themselves. That such effects are not inconsequential is shown by numerical solutions of Burger's equation,[9] and by Blackstock's[12] use of the dual frequency Bessel-Fubini series[13] (which holds in an inviscid or weakly viscous fluid prior to the critical range at which shock formation occurs) to demonstrate the "absorption of sound by sound," which is a direct consequence of cross coupling between the primary wave fields.

In a subsequent paper, Merklinger, Mellen, and Moffett[14] derived a more sophisticated taper function for spherically spreading monofrequency waves, which unlike the previous function, includes the effect of viscous absorption on the phase advance of the peak amplitude. This function was obtained from an ordinary nonlinear differential equation of the Bernoulli form,[15] which Merklinger[16,17] originally deduced by quasi analytical arguments in order to provide a finite-amplitude taper for plane monofrequency waves. Actually, Merklinger's equation[16,17] had previously been deduced by Westervelt[18] and solved by Wiener[19] for the case of finite-amplitude standing waves. Furthermore, it is easily shown that this equation is simply a reduced form of Burger's equation in the spectral domain for a monofrequency wave, when all self-generated harmonics higher than the second are neglected.

Nevertheless, substituting the taper functions shown in Table 1b (which also gives their integrated forms) in Eq. 1 leads to the approximate expressions outlined in Table Ic for the asymptotic far-field pressure of

TABLE 1b

Model	T_N	T_F
Mellen, Moffett[1,2]	Equal to T_F	$1\Big/\sqrt{1+[(\sigma_o/2)\sinh^{-1}(r/r_o)]^2}$
Merklinger, Mellen, Moffett[14]	Equal to T_F	$1\Big/\sqrt{1+(\sigma_o/2)^2[e^{\alpha_T r_o}\int_{r_o}^{r_o} e^{-4\alpha_o r'}\frac{dr'}{r'}\int_{r_o}^{r'} e^{2\alpha_o r''}\frac{dr''}{r''}]}$
Fenlon	Equal to T_F	$1\Big/\sqrt{1+(\sigma_o/2)^2[E_1(\alpha_T r_o)-E_1(\alpha_T r_o)]^2 e^{2\alpha_T r_o}}$
Modified Berktay, Leahy	$1\Big/\sqrt{1+(\sigma_o/2\alpha_T r_o)^2(1-e^{-\alpha_T r_o}}$	$1\Big/\sqrt{1+(\sigma_o/2)^2[E_1(\alpha_T r_o)-E_1(\alpha_T r)]^2}$
Bartram[5]	$1\Big/\{1+\pi(\sigma_o/2\alpha_T r_o)(1-e^{-\alpha_o r})\}$	——

TABLE 1c

$p_-(r)/p_o = (\omega_-/\omega_o)G(\sigma_o,\alpha_T r_o)(r_o/r)e^{-\alpha_- r}$; $p_{o1} = p_{o2}$; $\alpha_T r_o = 2\alpha_o r_o$

Model	$G(\sigma_o,\alpha_T r_o)$	$\lim G, \alpha_T r_o >> 1$ $\sigma_o\Delta >> 1$	$\lim G, \alpha_T r_o << 1$ $\sigma_o\Delta << 1$
Mellen, Moffett[1,2]	$\int_o^\infty \frac{(\sigma_o/2)\exp(-X)dX}{\{1+[(\sigma_o/2)\sinh^{-1}(X/\alpha_T r_o)]^2\}\sqrt{(\alpha_T r_o')^2 + X^2}}$	$\frac{\pi}{2}(\omega_-/\omega_o)$	Undefined
Merklinger, Mellen, Moffett[14]	$\int_o^\infty \frac{(\sigma_o/2)\exp(-X)dX}{\{1+(\sigma_o/2)^2[e^{\alpha_T r_o}\int_{r_o}^{r} e^{-4\alpha_o r'}\frac{dr'}{r'}\int_{r_o}^{r'} e^{2\alpha_o r''}\frac{dr''}{r''}]\}}$	$\frac{\pi}{2}(\omega_-/\omega_o)$	$\pi/2$
Fenlon	$(\omega_-/\omega_o)^{n-1}\tan^{-1}[(\sigma_o/2)E_1(\alpha_T r_o)\exp(\alpha_T r_o)]$; $n=1+\frac{\log_{10}(\Delta/\Delta')}{\log_{10}(\omega_o/\omega_-)}$	$\frac{\pi}{2}(\omega_-/\omega_o)$	$\pi/2$
Modified Berktay, Leahy	$\sqrt{(\omega_-/\omega_o)^2[\tan^{-1}\{(\sigma_o/2\alpha_T r_o)(1-e^{-\alpha_T r_o'})\}]^2+[\tan^{-1}\{(\sigma_o/2)E_1(\alpha_T r_o')\}]^2}$	$\frac{\pi}{2}(\omega_-/\omega_o)$	$\pi/2$
Bartram[5]	$(\pi/2)(\omega_-/\omega_o)\{1+(\pi/\Gamma_o)\ln(1+\frac{\Gamma_o}{\pi})$; $\Gamma_o = 2\sigma_o/\alpha_T r_o$	$\frac{\pi}{2}(\omega_-/\omega_o)$	$\pi/2$

a "partially saturated" parametric array; the so called "Modified Berktay-Leahy Model," derived by the author, being included for the sake of completeness. For $\sigma_o \Delta \ll 1$ these expression reduce, as required to those of Table Ia. It should be noted in this connection that although Bartram's model[5] has been included in Table Ic it is only valid for "absorption-limited arrays" ($\alpha_T r_o' \gg 1$) since it is not asymptotically matched for all values of $\alpha_T r_o$.

Referring to the expressions of Table Ic, the term "saturated" was previously used[1,2] to denote the fact that $p_-(r)/p_o$ becomes constant for $\sigma_o \Delta \gg 1$. This use of the term is misleading however, because even if $p_-'(r)/p_o$ becomes independent of p_o, $p_-(r)$ remains linearly dependent on p_o for all subsequent values of $\sigma_o \Delta$ (a parameter directly proportional to p_o) so that the system is in no way "saturated." Hence the term "partially saturated" has been used instead to denote the linear dependence of $p_-'(r)$ on p_o. Clearly, the continued dependence of $p_-'(r)$ on p_o is an unsatisfactory result, since it violates the nature of stable nondispersive nonlinear systems which eventually tend to approach well defined states of equilibrium, as demonstrated for example, by the results of Shooter, Muir, and Blackstock[20] for the case of monofrequency finite-amplitude waves. Thus $p_-'(r)$ must eventually approach "saturation" as p_o increases indefinitely.

In the final analysis, as Cary[21] has pointed out, the real weakness of the solutions outlined in Table Ic is that there is no criterion for determining the conditions under which they fail, nor is there any means of establishing the errors involved in neglecting all finite-amplitude loss mechanisms other than second harmonic generation.

For these reasons another approach is required. This will be the subject of the following section which makes use of Burgers' equation to determine the amplitude dependence of the asymptotic far-field pressure of a parametric array, and relies on the more general second-order nonlinear wave equation to determine its frequency response. Unlike the models outlined in Table Ic however, the effect of all possible spectral interactions on the far-field solution are included. Thus, the major assumptions on which the model is based can be stated as follows:

(1) As in the case of all previous models[1-5] the amplitude and frequency responses of the asymptotic far-field solution are assumed to be independent. This implies that the far-field difference-frequency pressure $p'_-(r)$ can be expressed symbolically in the form,

$$p'_-(r)/p_o = (\omega_-/\omega_o)^n F(\sigma_{1,2}, \alpha_T r_o)(r_o/r)e^{-\alpha_- r}, \quad 1 \leq n \leq 2.$$

(2) As in the case of all previous models[1-5] a nondispersive medium is also assumed.

1. THEORETICAL ANALYSIS

As shown by Blackstock[5] the propagation of one dimensional progressive finite-amplitude wave in nondispersive thermo viscous fluids can be described, correct to second-order terms, by means of Burgers' equation. Using a slightly modified form of Blackstock's[22] stretched coordinate system, this equation can be expressed in terms of the excess pressure p', normalized with respect to its peak value at the source p_o, for plane cylindrical, or spherically spreading waves as,

$$\frac{\partial P}{\partial \zeta} - P\,\frac{\partial P}{\partial t'} - (1/\Lambda)\,\frac{\partial^2 P}{\partial t'^2} = 0; \quad P = (r/r_o)^{\ell}(p'/p_o), \ (\ell = 0,\ 1/2,\ 1), \tag{2}$$

where the variables ζ, t' (each with the dimension of time) and the parameter Λ are functionally related to measurable parameters in Table II; the value of ℓ being determined by the type of wave under consideration, i.e., plane, cylindrical, or spherical, respectively.

TABLE II - Functional dependence of ζ, t' and Λ on r/r_o and t, for plane, cylindrical, or spherical waves; $\sigma_o' = (\beta p_o r_o/\rho_o c_o^3)$; $\Lambda_o = \sigma_o'/\delta r_o$.

Wave Type	ℓ	ζ/σ_o	t'	Λ
Plane	0	r/r_o	$t - (r/c_o)$	Λ_o
Cylindrical	1/2	$2[(r/r_o)^{1/2}-1]$	$t - (r-r_o)/c_o$	$\Lambda_o(1+\zeta/2\sigma_o')^{-1}$
Spherical	1	$\ln(r/r_o)$	$t - (r-r_o)/c_o$	$\Lambda_o \exp(-\zeta/\sigma_o')$

Now the plane wave form of Eq. 2 can be considerably simplified by means of the Hopf-Cole[23,24] transformation, which expresses P in terms of a new dependent variable ψ as,

$$P(\zeta,t') = (2/\Lambda_o)\frac{\partial}{\partial t'}\{\ln\psi(\zeta,t')\} \tag{3a}$$

or
$$\psi(\zeta,t') = \exp\{(\Lambda_o/2)\int_o^{t'} P(\zeta,t'')dt''\}. \tag{3b}$$

Substituting Eq. 3a in Eq. 2 results in the linear heat conduction equation,

$$\frac{\partial\psi}{\partial\zeta} - (1/\Lambda_o)\frac{\partial^2\psi}{\partial t'^2} = 0. \tag{4}$$

Taking the Fourier Transform of Eq. 4, and solving the ordinary differential equation thus formed gives,

$$\tilde{\psi}_\omega(\zeta) = \tilde{\psi}_\omega(o)e^{-\omega^2\zeta/\Lambda_o}, \tag{5}$$

where
$$\tilde{\psi}_\omega(\zeta) = \int_{-\infty}^{\infty}\psi(\zeta,t')e^{-j\omega t'}dt' \tag{6a}$$

and
$$\psi(\zeta,t') = \frac{1}{2\pi}\int_{-\infty}^{\infty}\tilde{\psi}_\omega(\zeta)e^{j\omega t'}d\omega. \tag{6b}$$

If Eq. 5 is substituted in Eq. 6b, $\psi(\zeta,t')$ becomes,

$$\psi(\zeta,t') = \frac{1}{2\pi}\int_{-\infty}^{\infty}\tilde{\psi}_\omega(o)e^{-\omega^2\zeta/\Lambda_o}\,d\omega, \tag{7}$$

where $\tilde{\psi}_\omega(o)$ is given by Eqs. 6a and 3b as,

$$\tilde{\psi}_\omega(o) = \int_{-\infty}^{\infty}\psi(o,t')e^{-j\omega t'}\,dt'$$

$$= \int_{-\infty}^{\infty} e^{(\Lambda_o/2)\int_o^{t'}P(o,t'')dt''}e^{-j\omega t'}dt'. \tag{8}$$

In the case of a parametric source operating simultaneously at angular frequencies ω_1 and ω_2, the normalized excess pressure at the source is given by the expression,

$$P(o,t) = P_{o1}\sin(\omega_1 t + \phi_1) + P_{o2}\sin(\omega_2 t + \phi_2);\ P_{oi} = (p_{oi}/p_o)(i = 1,2). \quad (9)$$

Substituting Eq. 9 in Eq. 8 and expressing the resulting exponent as a double Bessel function series of imaginary argument[25] gives,

$$\tilde{\psi}_\omega(o) = \sum_{n,m=-\infty}^{\infty}(-1)^{n+m} I_n(\Gamma_1/2) I_m(\Gamma_2/2) \int_{-\infty}^{\infty} e^{j(\omega_{nm}-\omega)t'} e^{j\phi_{nm}} e^{\{(\Gamma_1/2)\cos\phi_1 + (\Gamma_2/2)\cos\phi_2\}}$$

$$= 2\pi \sum_{n,m=-\infty}^{\infty}(-1)^{n+m} I_n(\Gamma_1/2) I_m(\Gamma_2/2)\delta(\omega_{nm}-\omega) e^{j\phi_{nm}} e^{\{(\Gamma_1/2)\cos\phi_1 + (\Gamma_2/2)\cos\phi_2\}}, \quad (10)$$

where the Dirac delta function $\delta(\omega)$ is defined as,[26]

$$\delta(\omega) = \frac{1}{2\pi}\int_{-\infty}^{\infty} e^{j\omega t'} dt' \quad (11)$$

with $$\omega_{nm} = (n\omega_1 + m\omega_2);\ \phi_{nm} = (n\phi_1 + m\phi_2);\ n,m = 0, \pm1, \pm2, \ldots \quad (12)$$

and $$\Gamma_i = (\Lambda_o/\omega_i)P_{oi} = (\beta p_{oi} k_i/\rho_o c_o^2 \alpha_i);\ (i = 1,2). \quad (13)$$

If Eq. 10 is substituted in Eq. 7, $\psi(\zeta,t')$ becomes,

$$\psi(\zeta,t') = \sum_{n,m=-\infty}^{\infty}(-1)^{n+m} I_n(\Gamma_1/2) I_m(\Gamma_2/2) e^{-\omega_{nm}^2\zeta/\Lambda_o} e^{j(\omega_{nm}t' + \phi_{nm})} - e^{\{(\Gamma_1/2)\cos\phi_1 + (\Gamma_2/2)\cos\phi_2\}}. \quad (14)$$

Returning to Eq. 3a and using Table I (with $\ell = o$) to replace ζ, $P(r,t')$ becomes,

$$P(r,t') = -(4/\Lambda_o)\frac{\sum_{n,m=o}^{\infty} a_{nm}\{\omega_{n,+m} e^{-\alpha_{n,+m} r}\sin(\omega_{n,+m}t' + \phi_{n,+m}) + \omega_{n,-m} e^{-\alpha_{n,-m} r}\sin(\omega_{n,-m}t' + \phi_{n,-m})\}}{1 + 2\sum_{n,m=o}^{\infty} a_{nm}\{e^{-\alpha_{n,+m} r}\cos(\omega_{n,+m}t' + \phi_{n,+m}) + e^{-\alpha_{n,-m} r}\cos(\omega_{n,-m}t' + \phi_{n,-m})\}} \quad (15)$$

where $$a_{nm} = (-1)^{n+m}\{\frac{I_n(\Gamma_1/2)I_m(\Gamma_2/2)}{I_o(\Gamma_1/2)I_o(\Gamma_2/2)}\}. \quad (16)$$

Inspection of Eq. 15 shows that each term in the double summations of the numerator and denominator decays exponentially at a rate dependent on its absorption coefficient. Since the latter is proportional to the frequency squared, it is clear that as r increases indefinitely the term with the smallest absorption coefficient (which in this instance is that of the difference frequency component $\omega_{1,-1}$ will outlive the others). Thus, the asymptotic form of Eq. 15 becomes,

$$P(r,t') \to -(4/\Lambda_o)\{\frac{a_{1,-1}\omega_- e^{-\alpha_- r}\sin(\omega_- t' + \phi_-)}{1 + 2a_{1,-1}\omega_- e^{-\alpha_- r}\cos(\omega_- t' + \phi_-)}\}, \quad \alpha_- r > 1 \quad (17a)$$

$$\simeq -(4/\Lambda_o)a_{1,-1}\omega_-\{e^{-\alpha_- r}\sin(\omega_- t' + \phi_-) - \frac{1}{2}e^{-2\alpha_- r}\sin 2(\omega_- t' + \phi_-) + \ldots\}, \quad (17b)$$

where $$\omega_- = \omega_{1,-1} \text{ and } \alpha_- = \alpha_{1,-1}. \quad (18)$$

At still greater ranges, only the first term of the distorted sine wave described by Eq. 17b survives, so that eventually,

$$P(r,t') \to P_-(r)\sin(\omega_- t + \phi_-), \quad \alpha_- r >> 1, \quad (19)$$

where $$P_-(r) = -(\omega_-/\omega_o)(4/\Gamma_o)e^{-\alpha_- r}; \quad \Gamma_o = (\Lambda_o/\omega_o); \quad \omega_o = \frac{1}{2}(\omega_1 + \omega_2) \quad (20a)$$

or

$$p'_-(r)/p_o = -(\omega_-/\omega_o)(2/\chi'_o)\{\frac{I_1(\chi'_1)I_1(\chi'_2)}{I_o(\chi'_1)I_o(\chi'_2)}\}e^{-\alpha_- r} \quad (20b)$$

with $$\chi'_i = \Gamma_i \text{ and } \chi'_o = \Gamma_o, \ (i = 1,2). \quad (21)$$

For small values of χ'_i, Eq. 20b becomes,

$$p'_-(r)/p_o = -(\omega_-/\omega_o)\{\frac{\chi'_1\chi'_2}{2\chi'_o}\}e^{-\alpha_- r}, \quad \chi_i << 1, \quad (i = 1,2) \tag{22a}$$

or
$$p'_-(r) = (K/2)p_{o1}p_{o2}(k_-/\alpha_T)e^{-\alpha_- r} \tag{22b}$$

where
$$K = \beta/\rho_o c_o^2. \tag{23}$$

As shown in Appendix A, Eq. 22b is the asymptotic far-field form of the unsaturated (pre shock) plane wave solution of Burgers' equation (Eq. 2) derived by Naugol'nykh, Soluyan and Khokhlov.[27]

Alternatively, for spherically spreading waves centered at range r_o, since $P_-(r) = rp'_-(r)/r_o p_o$, the asymptotic far-field solution which corresponds to Eq. 20b, can be expressed as,

$$p'_-(r)/p_o = -(\omega_-/\omega_o)(2/\chi''_o)\{\frac{I_1(\chi''_1)I_1(\chi''_2)}{I_o(\chi''_1)I_o(\chi''_2)}\}(r_o/r)e^{-\alpha_- r}. \tag{24}$$

For small values of χ''_i, Eq. 24 becomes,

$$p'_-(r)/p_o = -(\omega_-/\omega_o)\{\frac{\chi''_1\chi''_2}{2\chi''_o}\}(r_o/r)e^{-\alpha_- r}, \quad \chi''_i << 1, \quad (i = 1,2). \tag{25}$$

Equating this expression to the asymptotic far-field form of the unsaturated (pre shock) spherical wave solution of Burgers' equation (Eq. 1), as specified by Eq. A-19 of Appendix A, χ''_i and χ''_o become,

$$\chi''_i = \sigma_i E_1(\alpha_T r_o); \quad \chi''_o = \sigma_o E_1(\alpha_T r_o), \quad (i = 1,2). \tag{26}$$

Up to this point the discussion has been confined to asymptotic far-field solutions of Burgers' equation for infinitely plane and spherical wave fields. However, these particular solutions can be combined to obtain an expression for the asymptotic far-field form of the difference-frequency signal generated in the medium by a dual frequency parametric source of finite dimensions.

For such sources unsaturated (pre shock) solutions of the three dimensional nonlinear wave equation obtained by Muir[28] and Blue[29] and the author,[3] show that if the parametric interaction takes place primarily within the collimation distance r_o, the difference-frequency pressure is proportional to ω_-^2 in contrast to the dependence on ω_- predicted by Eqs. 20a and 20b. A heurestic explanation of this discrepancy, due to Mellen and Moffett,[1] is that in the case of a bounded source, the difference-frequency field, like the primary waves, has a collimation distance r_{o_-} which is shorter than r_o on account of its longer wavelength, i.e., $r_{o_-} = S_o/\lambda_- = r_o(\omega_-/\omega_o)$. Thus, if the near-field primary wave absorption loss ($\alpha_T r_o$) is such that nonlinear interaction occurs primarily within r_o, the difference-frequency pressure field described by Eq. 20b (which applies to infinite plane waves) must be modified to include the influence of spherical spreading losses, so that it becomes,

$$|p'_-(r)/p_o| = (\omega_-/\omega_o)(2/\chi'_o)\left\{\frac{I_1(\chi'_1)I_1(\chi'_2)}{I_o(\chi'_1)I_o(\chi'_2)}\right\}(r_{o_-}/r)e^{-\alpha_- r}$$

$$= (\omega_-/\omega_o)^2(2/\chi'_o)\left\{\frac{I_1(\chi'_1)I_1(\chi'_2)}{I_o(\chi'_1)I_o(\chi'_2)}\right\}(r_o/r)e^{-\alpha_- r}, \quad \alpha_T r_o > 1 \qquad (27)$$

where χ'_i and χ_o are defined by Eq. 21.

Alternatively, if the near-field primary wave absorption loss ($\alpha_T r_o$) is very small, most of the nonlinear interaction takes place beyond r_o, so that if the contribution to the difference-frequency field generated within r_o is neglected, the asymptotic far-field solution is given by Eq. 20b, which is reexpressed here for the benefit of the reader as,

$$|p'_-(r)/p_o| = (\omega_-/\omega_o)(2/\chi''_o)\{\frac{I_1(\chi''_1)I_1(\chi''_2)}{I_o(\chi''_1)I_o(\chi''_2)}\}(r_o/r)e^{-\alpha_- r}, \quad \alpha_T r_o < 1, \qquad (28)$$

where χ''_i and χ''_o are defined by Eq. 26.

In the general case, when both the near and far-fields of the primary waves contribute significantly to the nonlinear interaction process, a combined form of Eqs. 27 and 28 can be expressed as,

$$|p'_-(r)/p_o| = (\omega_-/\omega_o)^n(2/\chi_o)\{\frac{I_1(\chi_1)I_1(\chi_2)}{I_o(\chi_1)I_o(\chi_2)}\}(r_o/r)e^{-\alpha_- r}, \quad 1 \leq n \leq 2, \qquad (29)$$

where χ_i, χ_o and n are obtained by matching the unsaturated forms of the asymptotic solutions (for $\alpha_T r_o$ greater than and less than unity) defined by Eqs. 27 and 28, as shown in Appendix B. Thus,

$$\chi_i = \sigma_i \Delta, \; \chi_o = \sigma_o \Delta, \quad (i = 1,2) \qquad (30)$$

where $$\Delta = E_1(\alpha_T r_o)e^{\alpha_T r_o} \to 1/\alpha_T r_o, \text{ for } \alpha_T r_o > 1. \qquad (31)$$

Likewise, $$n = 1 + \{\frac{\log_{10}(\Delta/\Delta')}{\log_{10}(\omega_o/\omega_-)}\}, \qquad (32)$$

where $$\Delta' = E_1(\alpha_T r'_o)e^{\alpha_T r'_o} \to 1/\alpha_T/r'_o, \text{ for } \alpha_T r'_o > 1; \; r'_o = r_o(\omega_o/\omega_-). \qquad (33)$$

It is clear from inspection of Eq. 32, with the aid of Eqs. 31 and 33, that the index n approaches unity for $\alpha_T r_o < 1$, and approaches the value two, for $\alpha_T r_o > 1$, as required. The index n, which defines the frequency response of a parametric array is shown in Fig. 3 as a function of $\alpha_T r_o$ for different values of the "frequency downshift ratio" ω_o/ω_-. Likewise, the parameter Δ, defined by Eq. 31 can easily be obtained from Fig. 2, which gives Δ', as a function of $\alpha_T r'_o$. For small values of χ_i, Eq. 29 can be reexpressed with the aid of Eqs. 30 to 33, 21 and 26 as,

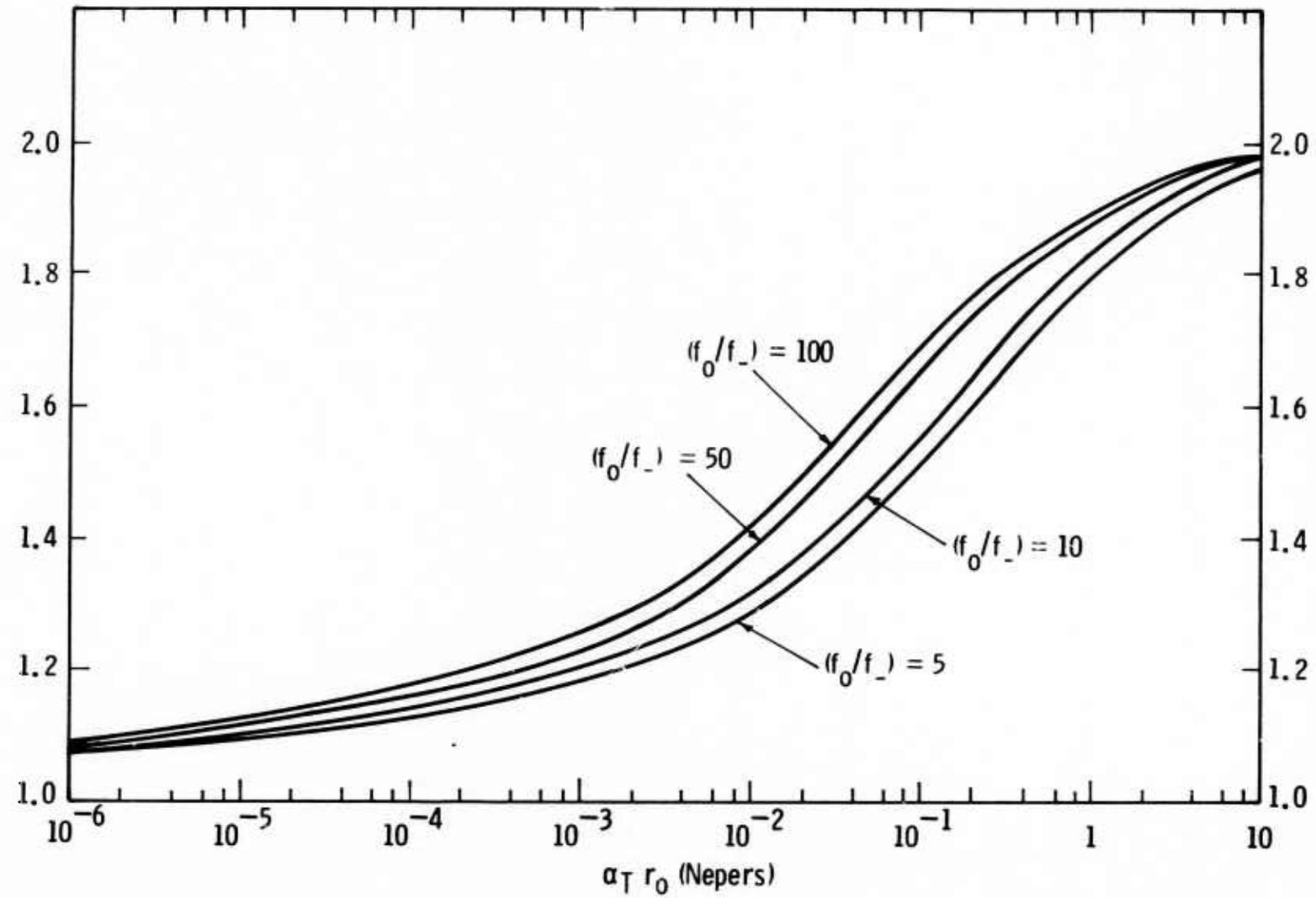
2.0
1.8
1.6
1.4
1.2
1.0
$(f_0/f_-) = 100$
$(f_0/f_-) = 50$
$(f_0/f_-) = 10$
$(f_0/f_-) = 5$
10^{-6}
10^{-5}
10^{-4}
10^{-3}
10^{-2}
10^{-1}
1
10
$\alpha_T r_0$ (Nepers)

Fig. 3

$$|p'_-(r)/p_o| = (\omega_-/\omega_o)^n\{(\sigma_{1,2}/2)E_1(\alpha_T r_o)\exp(\alpha_T r_o)\}(r_o/r)e^{-\alpha_- r}, \ \chi_i << 1, \ (i = 1,2) \tag{34}$$

$$\rightarrow (\omega_-/\omega_o)^2(\sigma_{1,2}/2\alpha_T r_o)(r_o/r)e^{-\alpha_- r}, \ \alpha_T r_o >> 1 \tag{34a}$$

$$\rightarrow (\omega_-/\omega_o)(\sigma_{1,2}/2)E_1(\alpha_T r_o)(r_o/r)e^{-\alpha_- r}, \ \alpha_T r_o << 1 \tag{34b}$$

where Eqs. 34a and 34b are the unsaturated forms of Eqs. 27 and 28, respectively, as required. Eq. 34a is Westervelt's[7] unsaturated (pre shock) asymptotic far-field solution for an "absorption limited" parametric array (where the nonlinear interaction takes place primarily within the near field of the primary waves), and Eq. 34b is the equivalent pre shock asymptotic solution derived by Cary[8] and the author[8,9] for a "spreading loss limited" parametric array (where the nonlinear interaction takes place primarily in the far-field of the primary waves). Equation 34 which combines these unsaturated (pre shock) asymptotic solutions is equivalent to Eq. B-4 of Appendix B as previously exhibited in Table Ia and in Fig. 2, where it was shown to be in good agreement with the alternative approximations derived by Mellen and Moffett,[1,2] Berktay and Leahy.[4]

The subject of this paper however, is the more general Eq. 29 which includes the unsaturated (pre shock) solution represented by Eq. 34 as a special case. If $\chi_1 = \chi_2 = \chi$, Eq. 29 becomes,

$$|p'_-(r)| = (\omega_-/\omega_o)^n(2/Kk_o\ell)\{\frac{I_1(\chi)}{I_o(\chi)}\}^2 \frac{e}{r}^{-\alpha_- r}; \ K = \beta/\rho_o c_o^2 \tag{35a}$$

$$\rightarrow (\omega_-/\omega_o)^n(1/2Kk_o\ell)\chi^2 \frac{e}{r}^{-\alpha_- r} = (\omega_-/\omega_o)^n(Kk_o\ell)(p_{1,2}r_o)^2 \frac{e}{r}^{-\alpha_- r}, \ \chi << 1 \tag{35b}$$

where $\chi = (Kk_o p_{1,2} r_o)\Lambda$; $p_{1,2} = p_{o1} = p_{o2}$. (36)

In this form, the amplitude dependence of the asymptotic far-field solution is controlled by the function $\{I_1(\chi)/I_o(\chi)\}^2$, which as shown in Fig. 4 resembles the well known characteristic of a simple two plate vacuum tube, passing from a square law dependence on the mean primary wave amplitude $p_{1,2}$ through a lower power dependence, to complete independence or saturation at high values of χ(or $p_{1,2}$).

In addition to defining the far-field amplitude and frequency response of a parametric array, Eqs. 29 and 32 can also be used to determine the far-field directivity function for the case of a "spreading loss limited" array, by means of Lockwood's approximation,[30] as previously utilized by the author.[13] This consists in replacing χ_i in Eq. 29 by $\chi_i D_i(\theta,\phi)$, where $D_i(\theta,\phi)$ $(i = 1, 2)$ are the normalized far-field directivity functions of the individual primary waves, respectively. If for example, $\chi_1 = \chi_2$, and $\alpha_T r_o = 10^{-3}$Np, the far-field difference-frequency directivity function generated in the medium by a circular piston source with $k_o a = 10$, and $f_o/f_- = 10$ is depicted in Fig. 5 as χ varies by orders of magnitude from 0.1 to 10^3, respectively. These results show that as χ increases the difference-frequency beam pattern becomes blunted around the axis and the sidelobe levels increase relative to the major lobe until $\chi = 10^3$ when the beam becomes essentially omnidirectional. This phenomenon which has been discussed and confirmed experimentally by Lockwood, Muir and Blackstock[31] for monofrequency sources, is due to the dependence of finite-amplitude absorption on the primary wave amplitudes. Since these

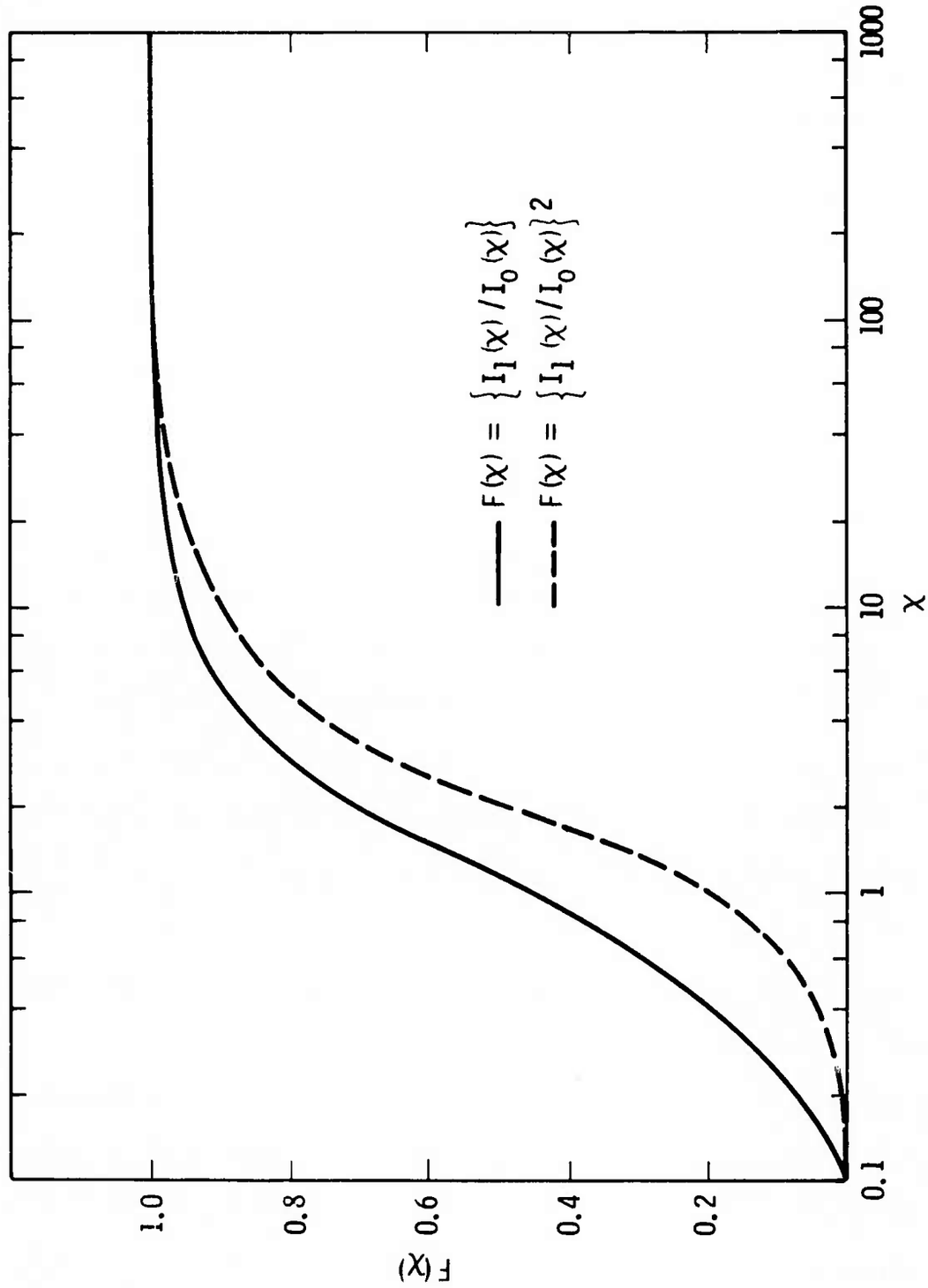

Fig. 4

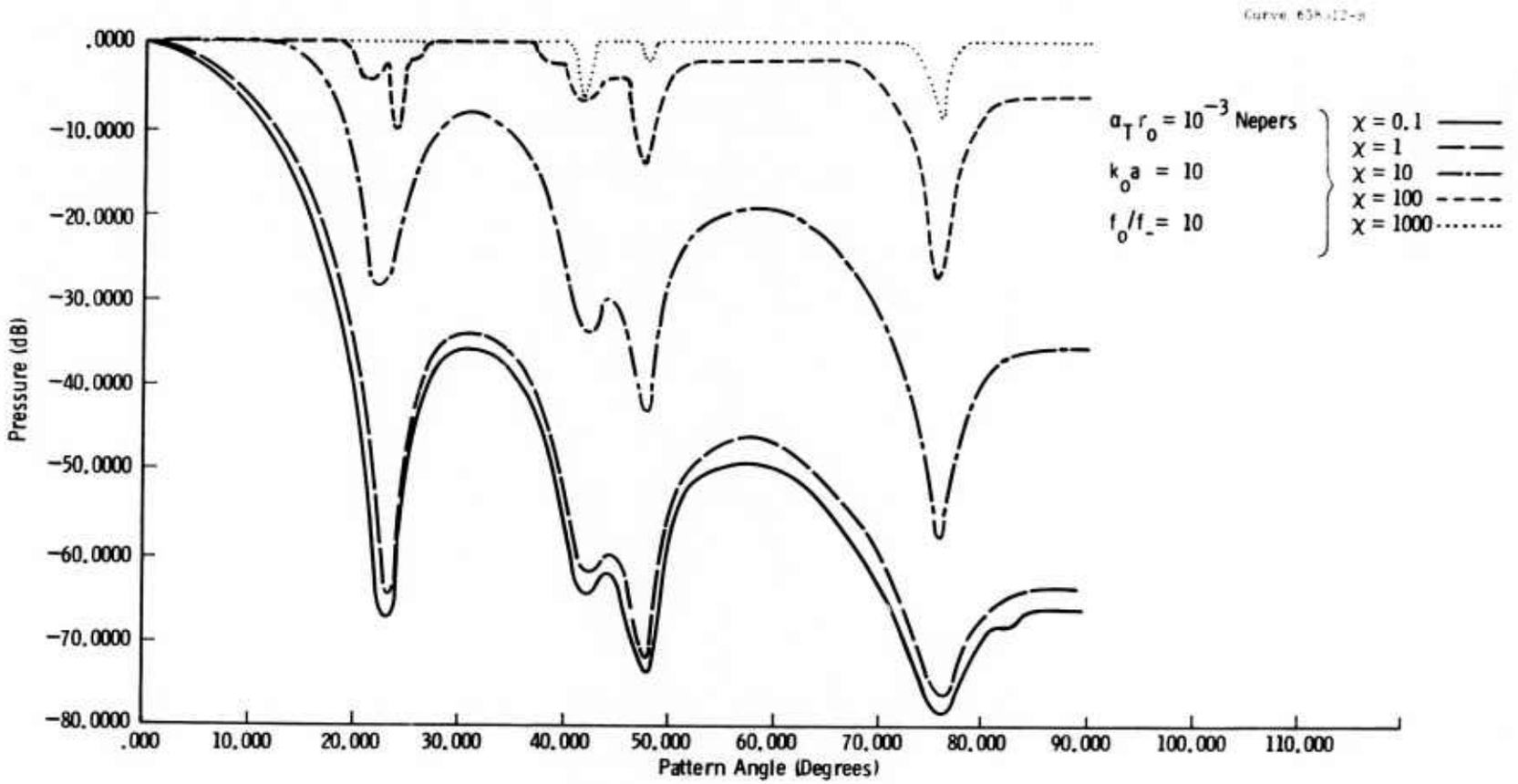
Curve 638-12-a
.0000
-10.0000
-20.0000
-30.0000
-40.0000
-50.0000
-60.0000
-70.0000
-80.0000
Pressure (dB)
.000
10.000
20.000
30.000
40.000
50.000
60.000
70.000
80.000
90.000
100.000
110.000
Pattern Angle (Degrees)
$\alpha_T r_o = 10^{-3}$ Nepers
$k_o a = 10$
$f_o/f_- = 10$
$\chi = 0.1$
$\chi = 1$
$\chi = 10$
$\chi = 100$
$\chi = 1000$

Fig. 5

are greatest on-axis in the far-field of a directive source, the amount of finite-amplitude absorption is also greatest on-axis, and decreases off-axis as determined by the primary wave directivity functions.

In contrast to the above case of a "spreading loss limited" parametric array ($\alpha_T r_o << 1$), no satisfactory expression for the directivity function of an absorption controlled array ($\alpha_T r_o >> 1$) as a function of χ has yet been obtained. However, it follows from Fig. 4 that it should be possible to use either Merklinger's approximation,[32] as discussed by Childs,[33] or Bartram's series approximation,[5] for values of χ less than 100, where complete saturation occurs.

Having thus obtained a general solution for the asymptotic far-field pressure of a parametric array, the next section will consider the construction of simple scaling laws from this solution to facilitate the design of parametric arrays.

2. PARAMETRIC SCALING LAWS

The asymptotic far-field pressure of a parametric array, derived in the previous section, can be expressed in terms of rms quantities (denoted by a bar) by writing Eqs. 29 to 31 in the form,

$$|\bar{p}_-'(r)/\bar{p}_o| = (1/\sqrt{2})(f_-/f_o)^n F(\bar{\chi}_o,\chi_1,\chi_2)(r_o/r)e^{-\alpha_- r}, \tag{37}$$

where $$F(\bar{\chi}_o,\chi_1,\chi_2) = (2/\bar{\chi}_o)\{\frac{I_1(\chi_1)I_1(\chi_2)}{I_o(\chi_1)I_o(\chi_2)}\} \tag{38}$$

and $$\bar{\chi}_o = \bar{\sigma}_o\Delta;\ \bar{\sigma}_o = Kk_o\bar{p}_o r_o;\ K = \beta/\rho_o c_o^2 \tag{39a}$$

with $$\chi_i = \sigma_i\Delta;\ \sigma_i = Kk_o p_{oi} r_o = \sqrt{2}\ Kk_o\bar{p}_{oi}r_o;\ (i=1,2), \tag{39b}$$

the index n being defined by Eqs. 32 and 33.

Let $$SL_- = 20\ \log_{10}|\bar{p}'(r)\cdot r\exp(\alpha_- r)| \tag{40a}$$

and $$SL_o = 20\ \log_{10}|\bar{p}_o r_o| \text{ with } SL_i = 20\ \log_{10}|\bar{p}_{oi}r_o|;\ (1=1,2), \tag{40b}$$

where $$SL_o = SL_i + 10\ \log_{10}(\frac{p_{o1}^2 + p_{o2}^2}{p_i^2});\ (i=1,2) \tag{41}$$

SL_-, SL_o, and SL_i (i=1,2) are thus the source levels referred to 1 m of the difference-frequency signal, the combined primary wave fields, and the individual primary waves, respectively.

Expressing Eq. 37 in logarithmic form with the aid of Eqs. 40 and 41 thus gives the conversion efficiency of the parametric source $(SL_- - SL_o)$ as,

$$SL_- - SL_o = 20n \log_{10}(f_-/f_o) + 20 \log_{10}(F/\sqrt{2}) \qquad (42)$$

where F is defined by Eq. 38.

Since $\bar{\chi}_o$ and χ_i are required to evaluate F, it is convenient to express them also in logarithmic form so that Eqs. 39a and 39b become,

$$20 \log_{10}\bar{\chi}_o = SL_o + 20 \log_{10} f_o + 20 \log_{10} + 20 \log_{10}(N/\sqrt{2}) \qquad (43a)$$

$$20 \log_{10}\chi_i = SL_i + 20 \log_{10} f_o + 20 \log_{10} + 20 \log_{10} N; \ (i=1,2) \qquad (43b)$$

where $N = (2\sqrt{2}\pi\beta/\rho_o c_o^3)(10^3)$, for f_o in kHz. (44)

If $\bar{\chi}_o$, $\chi_i << 1$ then Eq. 42 becomes,

$$SL_- = SL_o + 20n \log(f_-/f_o) + 20 \log_{10}(\chi_1\chi_2/2\sqrt{2}\bar{\chi}_o)$$

$$= SL_1 + SL_2 + 20 \log_{10} f_- + 20 \log_{10}\Delta' + 20 \log_{10}(N/2),$$

from Eqs. 32, 34a, and 34b, (45)

where Eqs. 45 is the unsaturated solution in logarithmic form previously obtained by the author.[3]

Since Δ, as defined by Eq. 31 is a function of $\alpha_T r_o$ only, and N, as defined by Eq. 44 is a constant for a given fluid, it is evident from inspection of Eqs. 42, 43a, and 43b that by scaling the source levels to 1 kHz, according to the procedure introduced by Mellen, Konrad, and Browning,[34] the conversion efficiency $(SL_- - SL_o)$ can be redefined as a function of the scaled source level SL_o^* and the nondimensional parameters $\alpha_T r_o$ and f_o/f_-. Thus if

$$SL_-^* = SL_- + 20 \log_{10} f_o, \ f_o \text{ in kHz} \qquad (46a)$$

and if $SL_o^* = SL_o + 20 \log_{10} f_o$, $SL_i^* = SL_i + 20 \log_{10} f_o$, (i=1,2) (46b)

then Eqs. 42, 43a, and 43b become,

$$SL_-^* - SL_o^* = SL_- - SL_o = 20n \log_{10}(f_-/f_o) + 20 \log_{10}(F/\sqrt{2}) \quad (47)$$

$$20 \log_{10} \bar{\chi}_o = SL_o^* + 20 \log_{10} \Lambda + 20 \log_{10}(N/\sqrt{2}) \quad (48a)$$

$$20 \log_{10} \chi_i = SL_i^* + 20 \log_{10} \Lambda + 20 \log_{10} N, \ (i=1,2). \quad (48b)$$

Curves of the conversion efficiency ($SL_- - SL_o$) and SL_-^* obtained from Eqs. 38, 47 and 48 with SL_1 equal SL_2, are shown as functions of SL_o^* for particular values of f_o/f_- and $\alpha_T r_o$ in Figs. 6a, 6b, 7a, 7b, 8a, and 8b, where the medium is water ($20 \log_{10} N = 281$ dB//1μPa), all pressures being referred to 1 μPa. Using these scaled characteristics, parametric sonars with similar values of f_o/f_- and $\alpha_T r_o$, but with different operating frequencies and source dimensions can be compared as functions of the scaled source level SL_o^*.

At this point it is instructive to compare the conversion efficiency defined by Eqs. 38, 47, and 48 with results obtained from Mellen and Moffett's model.[1,2] Such a comparison is shown in Fig. 9 where $f_o/f_- = 10$ and $\alpha_T r_o$ varies from 1 to 10^{-3} Np. It should be noted that, unlike Figs. 6b, 7b, and 8b, the ordinate in Fig. 9 gives the conversion efficiency as ($SL_- - SL_{1,2}$) which is referred to the mean primary wave source level $SL_{1,2}$, in keeping with Mellen and Moffett's[1,2] presentation of their results. Likewise, the abscissa in Fig. 9 is given in terms of the scaled mean primary wave level $SL_{1,2}^*$. It follows therefore, from the discussion at the beginning of this paper that the

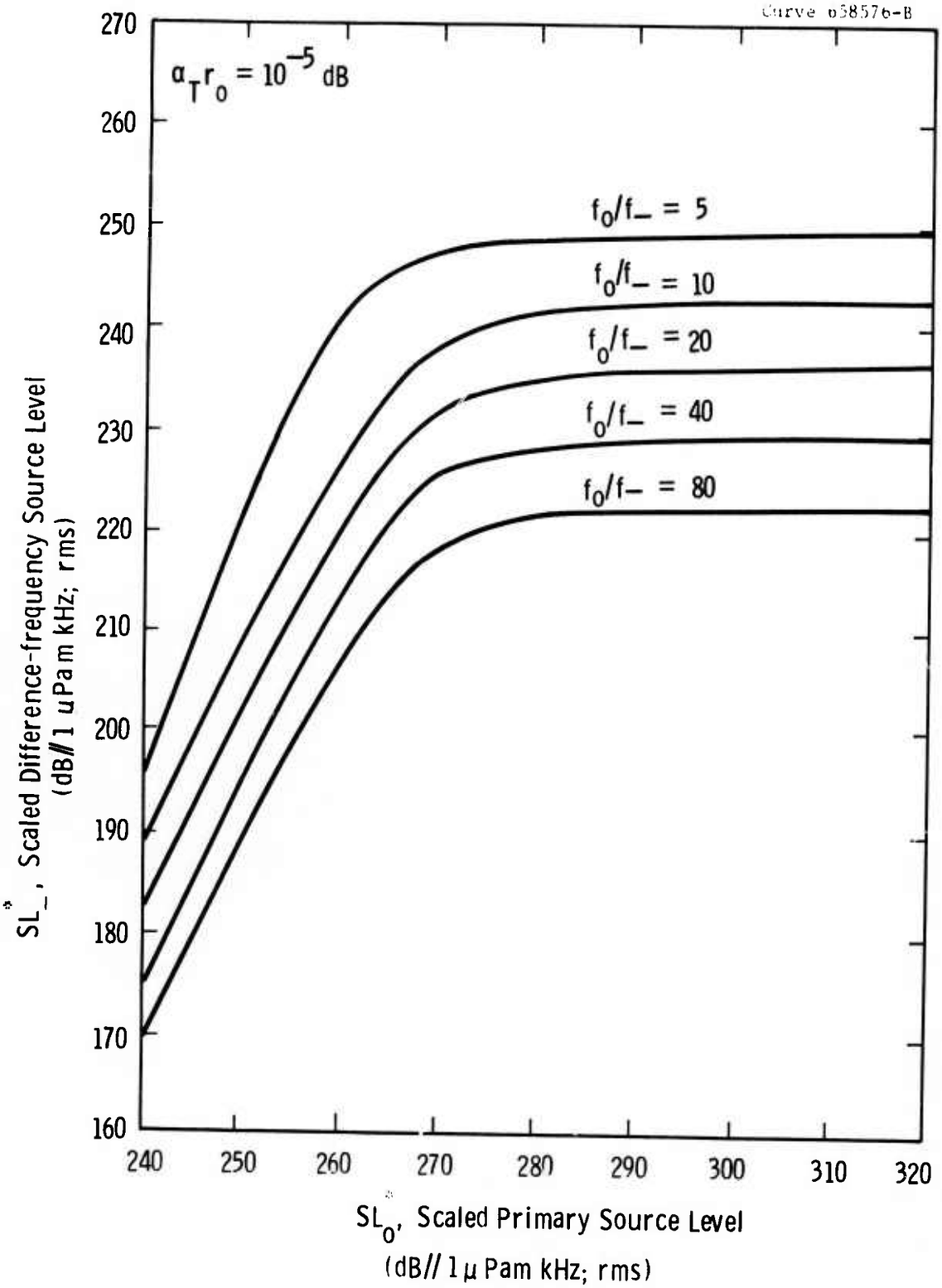
Curve 038576-B
$\alpha_T r_0 = 10^{-5}$ dB
$f_0/f_- = 5$
$f_0/f_- = 10$
$f_0/f_- = 20$
$f_0/f_- = 40$
$f_0/f_- = 80$
270
260
250
240
230
220
210
200
190
180
170
160
240
250
260
270
280
290
300
310
320
SL^*_-, Scaled Difference-frequency Source Level
(dB// 1 uPa m kHz; rms)
SL^*_0, Scaled Primary Source Level
(dB// 1 μ Pam kHz; rms)

Fig. 6a

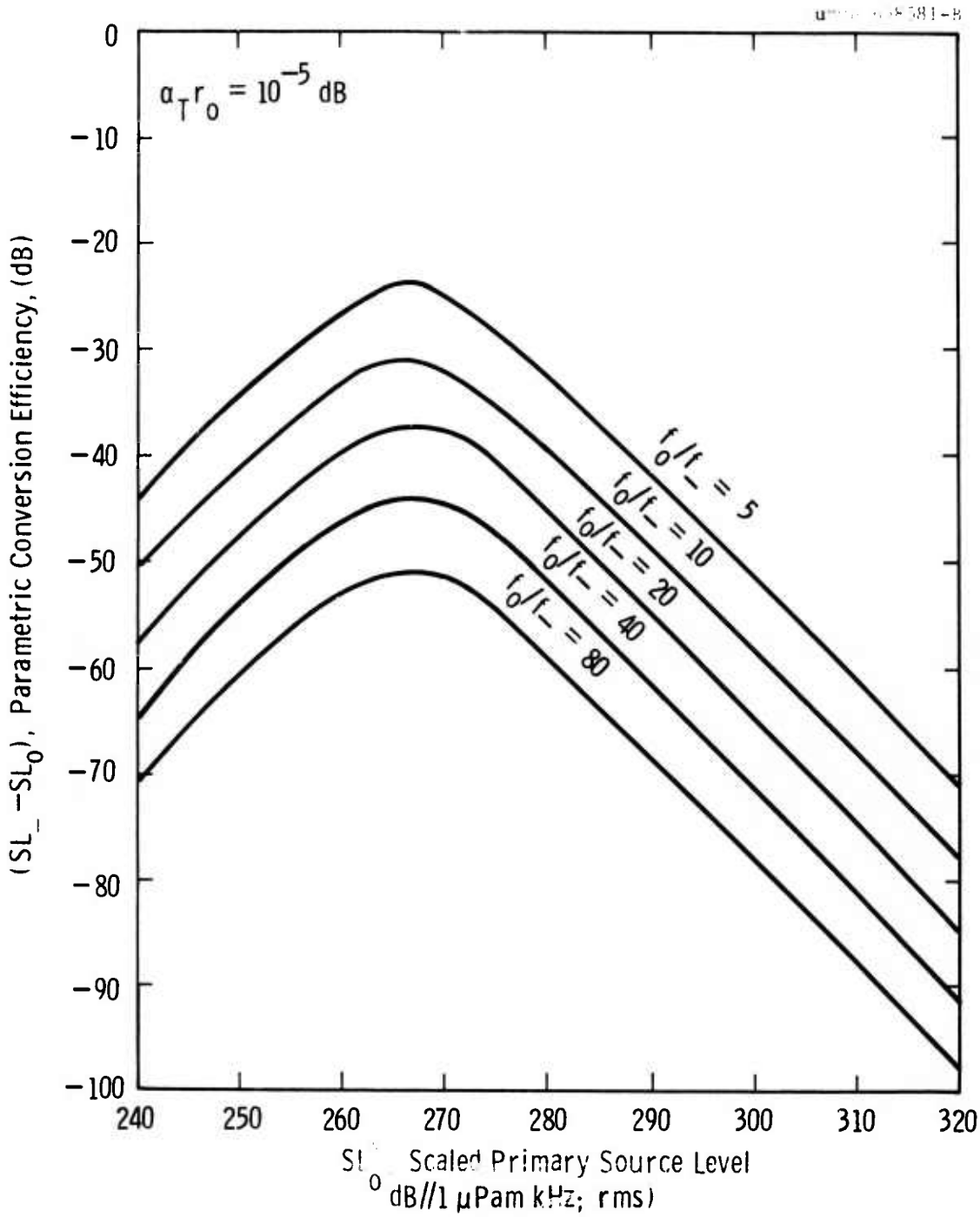
$\alpha_T r_o = 10^{-5}$ dB
$f_o/f_- = 5$
$f_o/f_- = 10$
$f_o/f_- = 20$
$f_o/f_- = 40$
$f_o/f_- = 80$
$(SL_- - SL_o)$, Parametric Conversion Efficiency, (dB)
0
−10
−20
−30
−40
−50
−60
−70
−80
−90
−100
240
250
260
270
280
290
300
310
320
SL_o Scaled Primary Source Level
dB//1 μPam kHz; rms)

Fig. 6b

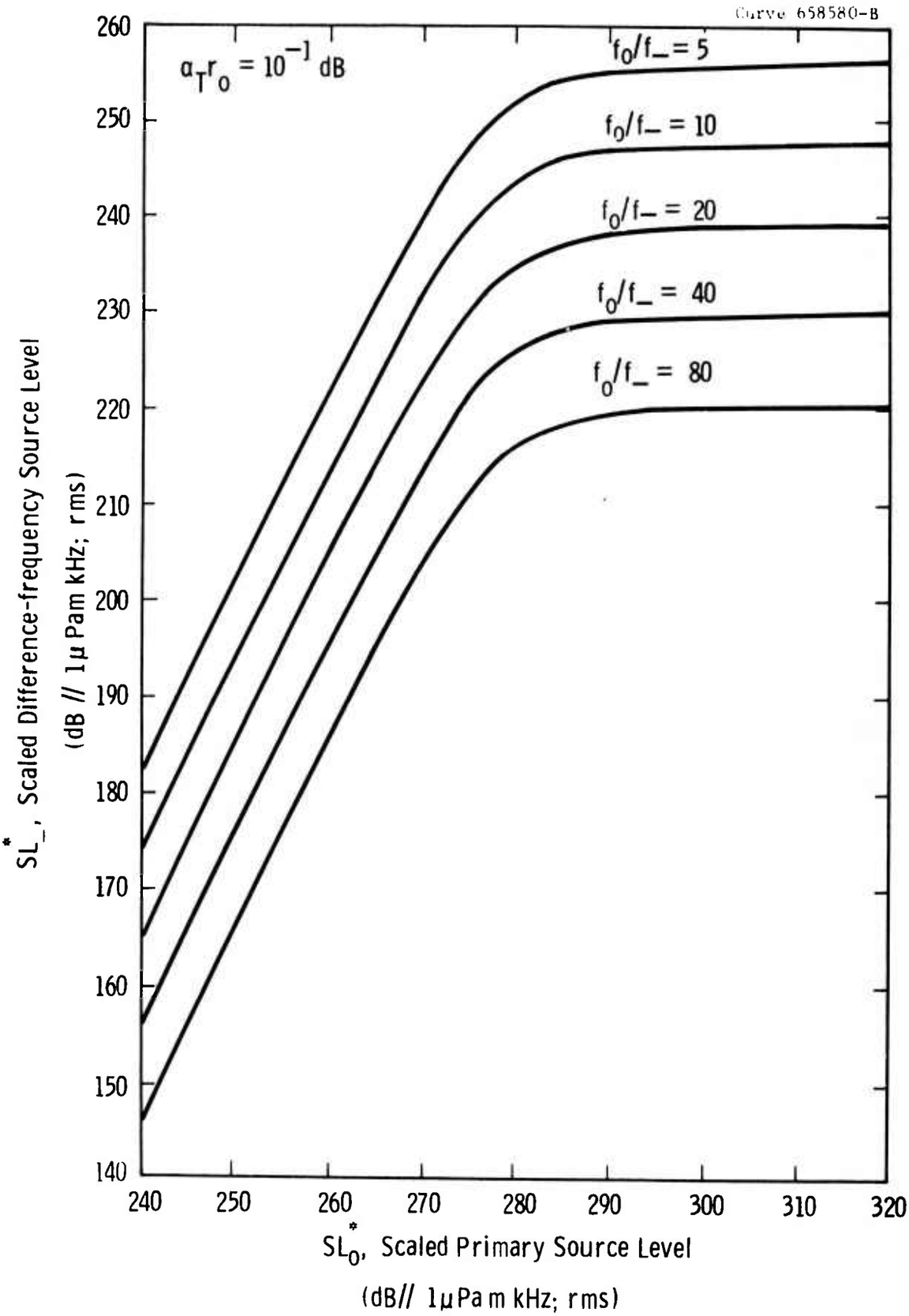
Curve 658580-B
$\alpha_T r_0 = 10^{-1}$ dB
$f_0/f_- = 5$
$f_0/f_- = 10$
$f_0/f_- = 20$
$f_0/f_- = 40$
$f_0/f_- = 80$
260
250
240
230
220
210
200
190
180
170
160
150
140
240
250
260
270
280
290
300
310
320
SL^*_-, Scaled Difference-frequency Source Level
(dB // 1μPam kHz; rms)
SL^*_0, Scaled Primary Source Level
(dB// 1μPa m kHz; rms)

Fig. 7a

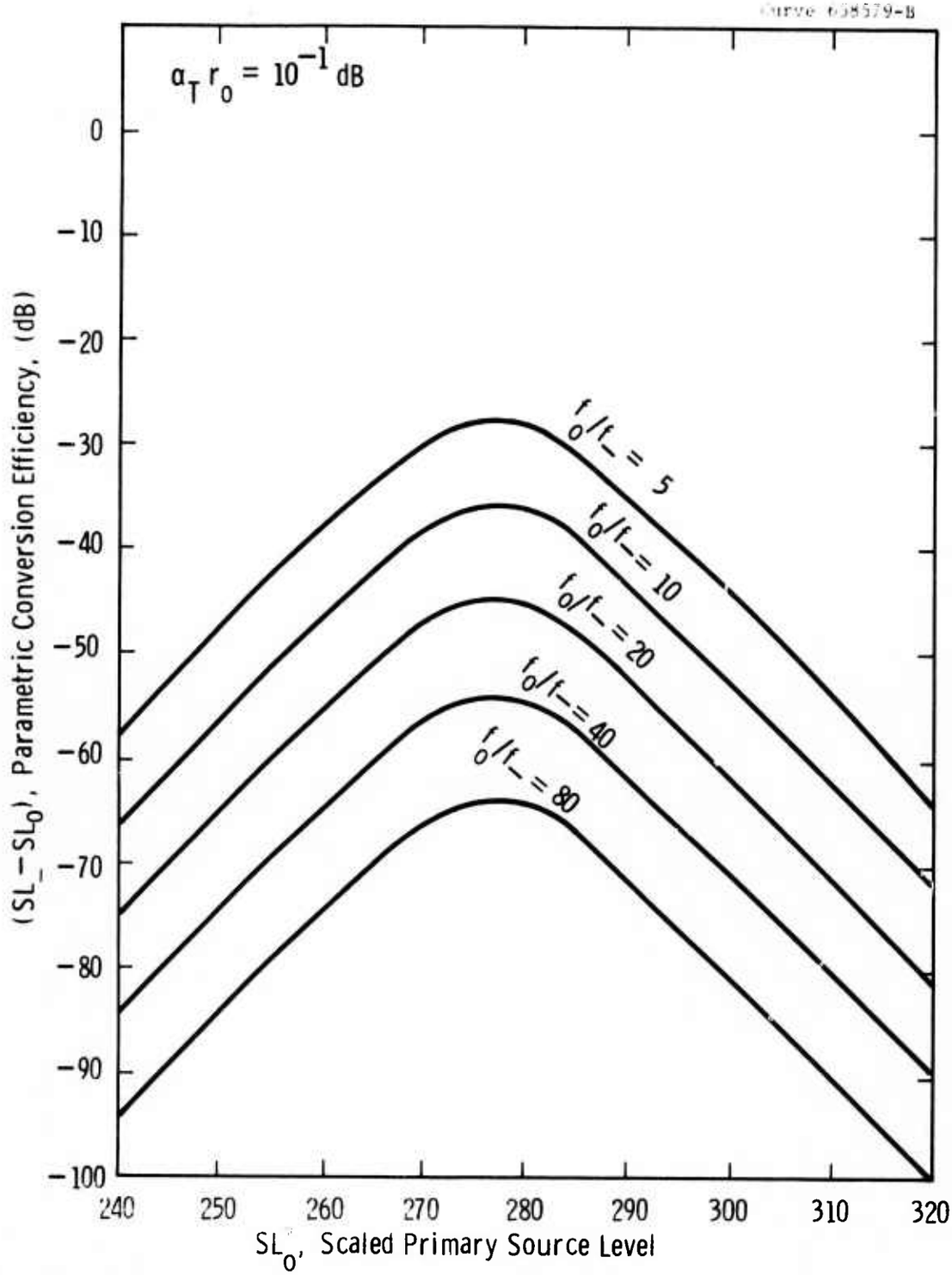
Curve 638579-B
$\alpha_T r_0 = 10^{-1}$ dB
0
−10
−20
−30
−40
−50
−60
−70
−80
−90
−100
$(SL_- - SL_0)$, Parametric Conversion Efficiency, (dB)
$f_0/f_- = 5$
$f_0/f_- = 10$
$f_0/f_- = 20$
$f_0/f_- = 40$
$f_0/f_- = 80$
240
250
260
270
280
290
300
310
320
SL_0, Scaled Primary Source Level
(dB // 1μ Pa m kHz; rms)

Fig. 7b

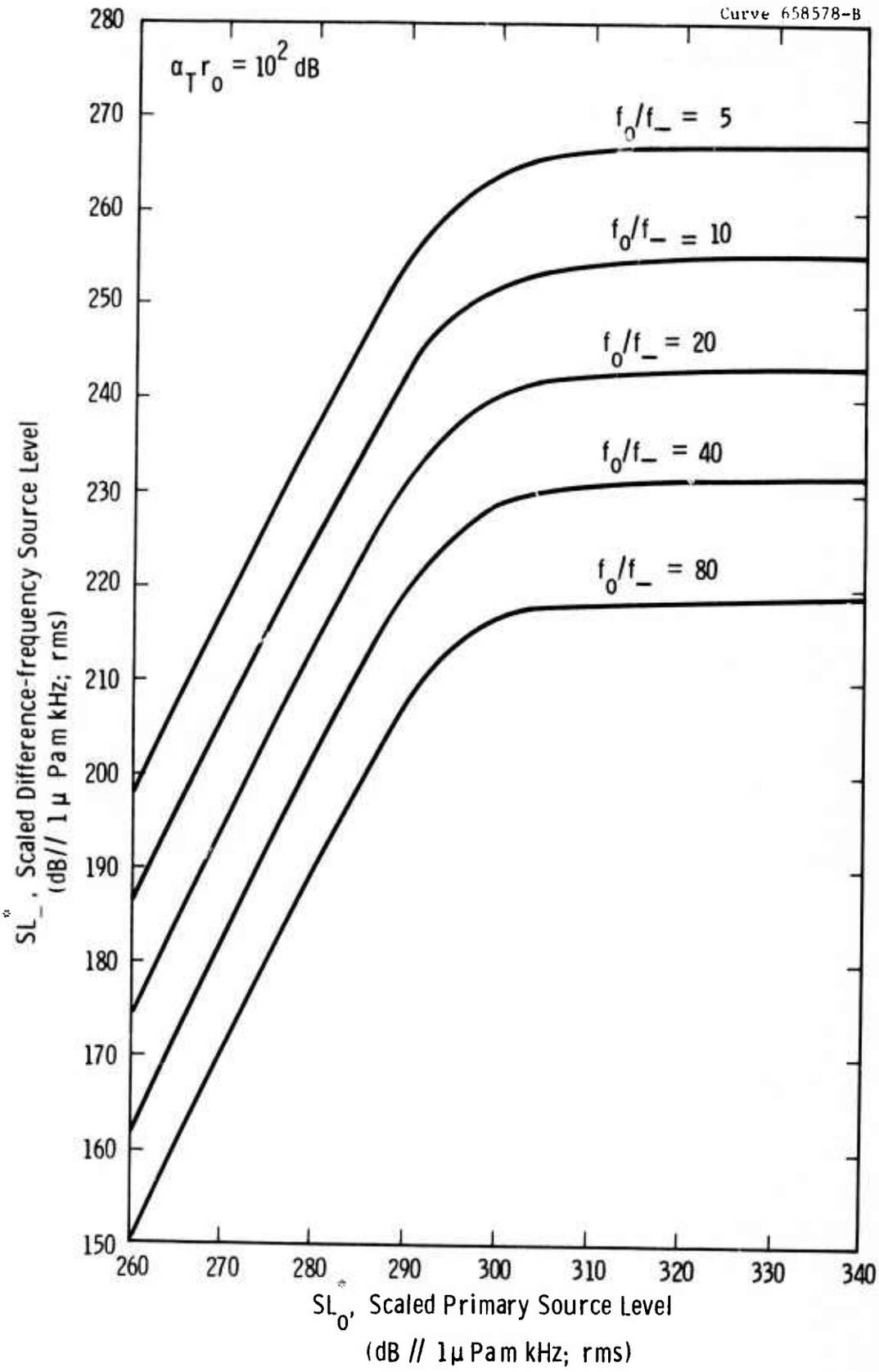
Curve 658578-B
$\alpha_T r_0 = 10^2$ dB
$f_0/f_- = 5$
$f_0/f_- = 10$
$f_0/f_- = 20$
$f_0/f_- = 40$
$f_0/f_- = 80$
280
270
260
250
240
230
220
210
200
190
180
170
160
150
260
270
280
290
300
310
320
330
340
SL_-^*, Scaled Difference-frequency Source Level
(dB// 1 μ Pa m kHz; rms)
SL_0^*, Scaled Primary Source Level
(dB // 1μ Pa m kHz; rms)

Fig. 8a

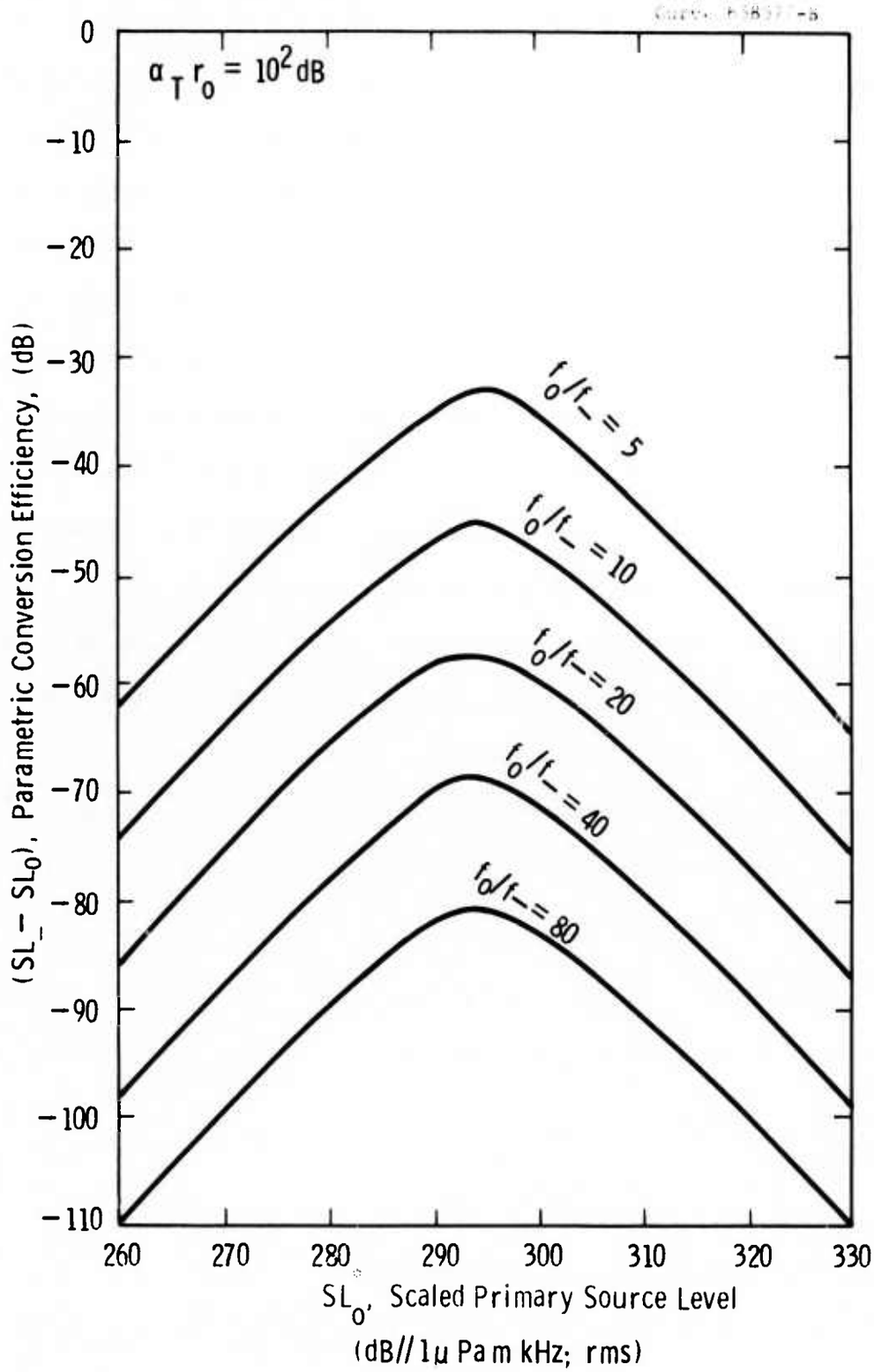
$\alpha_T r_0 = 10^2$ dB
$f_0/f_- = 5$
$f_0/f_- = 10$
$f_0/f_- = 20$
$f_0/f_- = 40$
$f_0/f_- = 80$
$(SL_- - SL_0)$, Parametric Conversion Efficiency, (dB)
0
−10
−20
−30
−40
−50
−60
−70
−80
−90
−100
−110
260
270
280
290
300
310
320
330
SL_0, Scaled Primary Source Level
(dB// 1μ Pa m kHz; rms)

Fig. 8b

difference between the results of the two models shown in Fig. 9, which becomes more accute as $SL^*_{1,2}$ increases, can be attributed entirely to the higher order spectral interactions neglected in Mellen and Moffett's model.[1,2] These interactions, which are taken into account in the model defined by Eqs. 38, 47, and 48, give rise to enhanced finite-amplitude losses, thus causing the conversion efficiency to decrease more rapidly (after its maximum value has been reached) as the primary wave source levels are increased. Numerical solutions of the spherical form of Burgers' equation (Eq. 2, $\ell = 1$) obtained with the aid of a computer program previously developed by the author[9] are also shown in Fig. 9 for $\alpha_T r_o \lesssim 10^{-2}$ Np, which defines the range of validity of the spherical wave model. Although extremely unstable and difficult to generate at high scaled source levels, these numerical solutions tend to confirm the trend of the analytical far-field model.

In order to further simplify the presentation of scaled results, a higher level of scaling can be introduced. Thus,

$$SL^{**}_- = SL^*_- + 20 \log_{10}\Lambda - 20n \log_{10}(f_-/f_o)$$

$$= SL_- + 20 \log_{10} f_o + 20 \log_{10}\Lambda - 20n \log_{10}(f_-/f_o) \quad (49a)$$

and if $SL^{**}_o = SL^*_o + 20 \log_{10}\Lambda$

$$= SL_o + 20 \log_{10} f_o + 20 \log_{10}\Lambda, \quad (49b)$$

then Eqs. 47 and 48 become,

$$SL^{**}_- - SL^{**}_o = (SL_- - SL_o) + 20n \log_{10}(f_o/f_-) = 20 \log_{10}(\Gamma/\sqrt{2}) \quad (50)$$

$$20 \log_{10}\bar{\chi}_o = SL^{**}_o + 20 \log_{10}(N/\sqrt{2}) \quad (51a)$$

$$20 \log_{10}\chi_i = SL^{**}_i + 20 \log_{10} N, \ (i=1,2). \quad (51b)$$

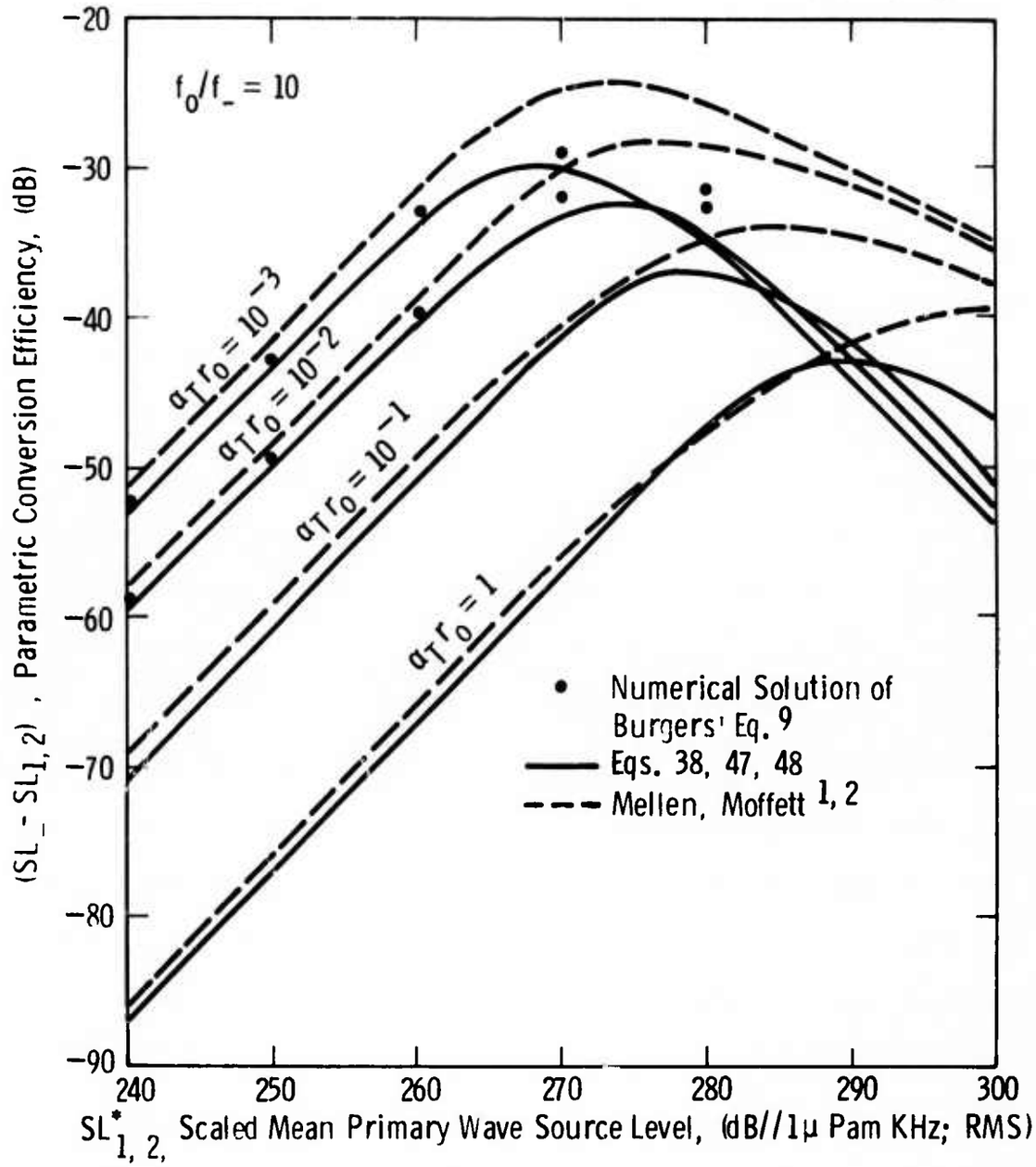
$f_0/f_- = 10$
$\alpha_T r_0 = 10^{-3}$
$\alpha_T r_0 = 10^{-2}$
$\alpha_T r_0 = 10^{-1}$
$\alpha_T r_0 = 1$
• Numerical Solution of Burgers' Eq. 9
Eqs. 38, 47, 48
Mellen, Moffett 1, 2
$(SL_- - SL_{1,2})$, Parametric Conversion Efficiency, (dB)
$SL^*_{1,2}$, Scaled Mean Primary Wave Source Level, (dB//1μ Pam KHz; RMS)
−20
−30
−40
−50
−60
−70
−80
−90
240
250
260
270
280
290
300

Fig. 9

Using Eqs. 38, 50, 51a, and 51b, $(SL_{-}^{**} - SL_{o}^{**})$ and SL_{-}^{**} can be evaluated as functions of SL_{0}^{**} to give the "universal" scaled characteristics shown in Figs. 10a and 10b. Experimental data obtained by a number of different investigators[34-38] under entirely different conditions with a variety of parametric sources, has been scaled and superimposed on these characteristics, showing reasonably good agreement despite the scatter. A summary of the source parameters used to obtain this data is given in Table III, which also includes values of $20 \log_{10}(\ell)$ calculated for the benefit of the reader from Eq. 33. With the exception of experiments 1, 2, 3, and 7 of Table III, the nearfield primary wave absorption loss $2\alpha_o r_o$ was given or could be calculated from reported values of α_o and r_o. Since experiments 1, 2, and 3 were performed in a hot salt water medium, Schulkin and Marsh's[39] expression for acoustic attenuation in sea water was used to calculate the values of α_o shown in Table III, based on an assumed temperature of 80°F with a salinity of 30 parts per thousand. In order to check the accuracy of these assumed conditions, the attenuation coefficient for experiment #4 (which was also conducted in the same salt water environment), was calculated using the same values of temperature and salinity to give the value $1.17(10^{-2})$Np/m shown in Table III. This calculation is in very good agreement with the value of $1.2(10^{-2})$ Np/m quoted by the investigators,[35] who also gave the attenuation coefficient for the 250 kHz source in experiment #2 as 10^{-2}Np/m in keeping with the calculated value of $0.95(10^{-2})$Np/m shown in Table III. In the case of experiment #7, since the medium was fresh water at normal temperature and pressure, α/f^2 was assumed to be $25(10^{-15})$Np secs^2/m.

300
290
280
270
260
250
240
260
270
280
290
300
310
320
330
SL_ (dB// 1 μPam kHz; rms)
SL$_0^{**}$ (dB// 1 μ Pam kHz; rms)

Fig. 10a

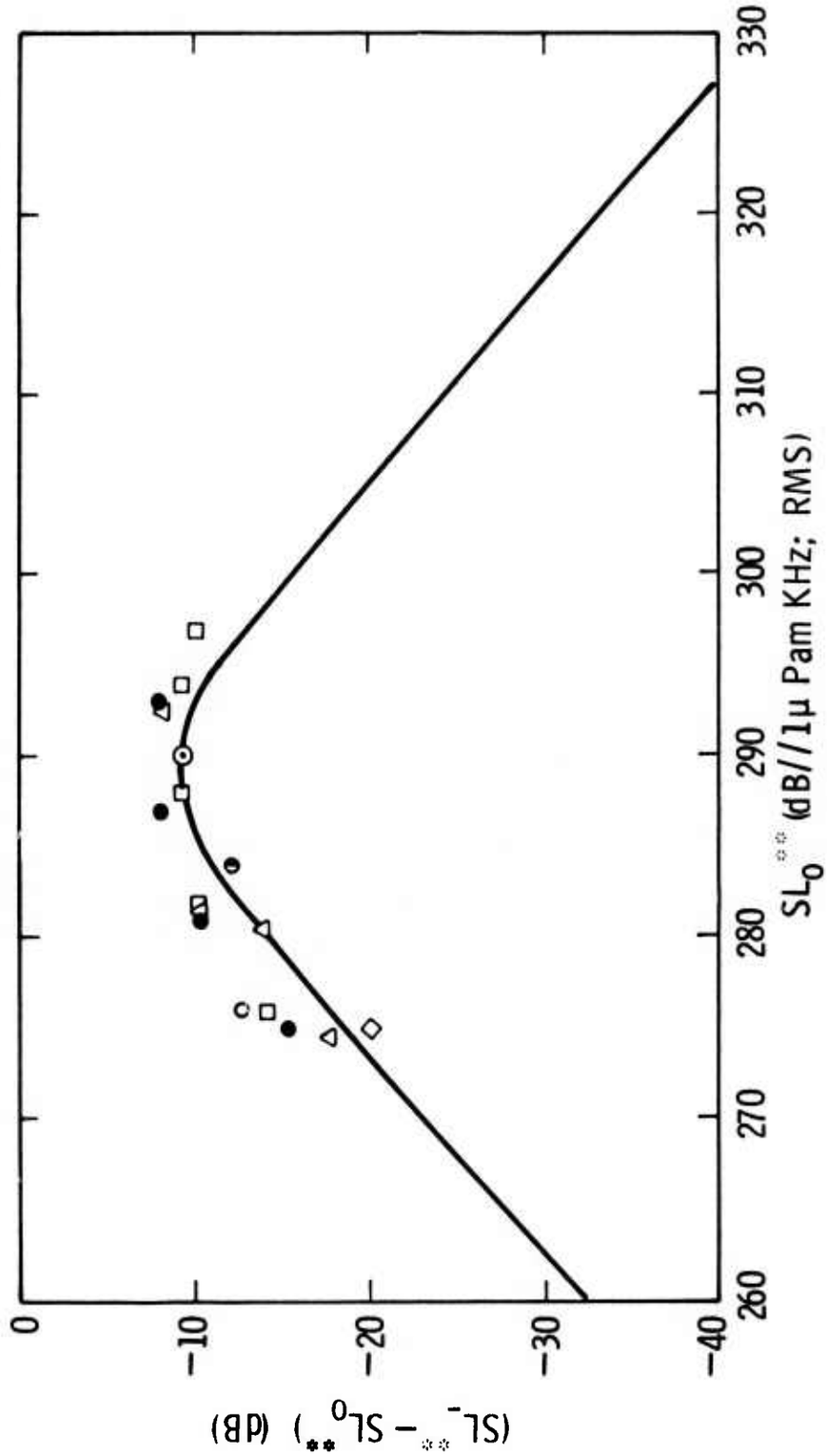
0
−10
−20
−30
−40
260
270
280
290
300
310
320
330
$(SL_{-}^{**} - SL_{0}^{**})$ (dB)
SL_{0}^{**} (dB//1μ Pam KHz; RMS)

Fig. 10b

TABLE III

#	Experiment	Legend	f_o kHz	α_o Np/m	r_o m	$2\alpha_o r_o$ Np	$20 \log_{10}(\Delta)$ dB
1	NUSC[34]	●	175	$6.76(10^{-3})$	16	$2.16(10^{-1})$	3.0
2	NUSC[34]	△	250	$0.95(10^{-2})$	8	$1.52(10^{-1})$	4.5
3	NUSC[34]	□	720	$2.08(10^{-2})$	4	$1.66(10^{-1})$	4.0
4	NUSC[35]	○	330	$1.17(10^{-2})$	0.25	$6.0(10^{-3})$	13.0
5	NUSC[36]	⊙	65	$2.23(10^{-3})$	28	$1.3(10^{-1})$	5.0
6	Muir and Willette[37]	◇	450	$6.25(10^{-3})$	1.4	$1.75(10^{-2})$	11.0
7	A. Eller[38]	◐	1435	$5.13(10^{-2})$	0.3	$3.09(10^{-3})$	14.0

An example of the calculations required to scale the data shown in Figs. 10a and 10b is given in Tables IVa and IVb for the case of the 250 kHz source listed as experiment #2 in Table III. The values of f_- given in Table IVa correspond to those of the experiment,[34] the values of 20 logΔ' being calculated from Eq. 33 with $\alpha_T r_o (\simeq 2\alpha_o r_o)$ as given in Table III. The index n is then calculated from Eq. 32. In Table IVb the actual measured values of SL_o and SL_- (for two different difference-frequencies) are reproduced, where the pressures are referenced to 1 μPa rather than 1 μbar, as used by the investigators.[34] These measurements are then scaled using Eqs. 46a, 46b, 49a, 49b, and Table IVa. Finally, the scaled difference-frequency levels are averaged to give $\langle SL_-^{**} \rangle$, on the grounds that the differences between them are caused by experimental inconsistencies which should disappear on the average.

Example: In order to use Figs. 10a and 10b to evaluate the effectiveness of a parametric array, consider the case of the 65 kHz source listed as experiment 5 in Table III, with $2\alpha_o r_o \simeq \alpha_T r_o = 0.13$ Np, and $20 \log_{10}\Delta = 5$ dB.

If, as was the case in the experiment[36] $SL_1 = SL_2 = 249$ dB//1 μPam; rms, then $SL_o = 251$ dB//1 μPam; rms, and from Eqs. 46b and 49b,

$$SL_o^{**} = SL_o + 20 \log_{10} f_o - 20 \log_{10} \quad ; \ f_o \text{ in kHz}$$

$$= 251 + 36 + 5$$

$$= 290 \text{ dB}.$$

TABLE IVa

f_- kHz	f_o/f_- -	$20 \log_{10}(\Delta')$ dB	n -	$20n \log_{10}(f_o/f_-)$ dB	$20 \log_{10}\{(f_o/f_-)^n(f_o\Delta)\}$ dB
12	20.8	-12	1.63	43	95.5
6	41.7	-17	1.66	54	106.5

TABLE IVb

Experimental Results[34]			Scaled Experimental Results				
SL_o dB	SL_-(12 kHz) dB	SL_-(6 kHz) dB	SL_o^{**} dB	SL_-(12 kHz) dB	SL_-^{**}(6 kHz) dB	$\langle SL_-^{**} \rangle$ dB	$\langle SL_-^{**} \rangle - SL_o^{**}$ dB
240	189	178	292.5	284.5	284.5	284.5	-8.0
234	181	170	286.5	276.4	276.4	276.4	-10.1
228	172	160	280.5	267.4	266.4	266.9	-13.6
222	160	150	274.5	255.4	256.4	255.9	-18.6

Thus, from Fig. 10a, $SL_{-}^{**} = 280.5$ dB. If, as in the experiment[36], $f_{-} = 3.5$ kHz, then from Eq. 33, $20 \log A' = -9$ dB; hence from Eq. 32, $n = 1.55$, with $20n \log_{10}(f_o/f_{-}) = 39.5$ dB. Finally, from Eqs. 46a and 49a,

$$SL_{-} = SL_{-}^{**} - (20 \log_{10} f_o + 20 \log_{10} A + 20 \log_{10}(f_o/f_{-})), \text{ or}$$

$$SL_{-}(3.5 \text{ kHz}) = 280.5 - (36 + 5 + 39.5)$$

$$= 200 \text{ dB, which is equal to the level obtained}$$

experimentally.[36] A very interesting result which follows directly from Eq. 50 and Fig. 10b is that the maximum conversion efficiency of a parametric source for a given frequency downshift ratio (f_o/f_{-}), can be expressed as,

$$(SL_{-} - SL_o)_{max} = -9 - 20n \log_{10}(f_o/f_{-}) \qquad (52)$$

where n, as defined by Eqs. 32 and 33, is a function of $\alpha_T r_o$ and $\alpha_T r_o'$. For the case of the 65 kHz source previously considered, the difference-frequency is 3.5 kHz and thus, $20n \log_{10}(f_o/f_{-}) = 39.5$ dB, so that the maximum conversion efficiency in this instance is -48.5 dB. Since the conversion efficiency obtained experimentally[36] was -51 dB for a source level of 251 dB, it follows that this sonar was operating close to its limit of maximum conversion efficiency.

CONCLUSIONS AND RECOMMENDATIONS

A new analytical model has been derived in this paper for calculating the asymptotic far-field pressure and conversion efficiency of a parametric array. Unlike previous models,[1-5] this new model includes the effect of all degenerative spectral interactions on the conversion efficiency of the parametric mixing process. Two levels of scaled performance characteristics have been derived from this analysis, which should simplify the problem of designing small scale model tank experiments to simulate the performance (and thus assist the design) of large scale parametric sonars.

The model has been shown to give good agreement with experimental data obtained by different investigators[34-38] over a wide range of experimental conditions. However, a word of caution must be added at this point concerning the comparison of data obtained in a dispersive medium such as sea water, with the predictions of analytical models derived from a nondispersive wave equation.

Unfortunately, most of the high amplitude data available in the literature[34,35] which was used to test the model derived in this paper, and all previous models,[1-5] was obtained in a salt water medium at primary wave frequencies between 175 kHz and 720 kHz. Since this range of frequencies lies within the 'resonant' region of the salt water relaxation process, the attenuation coefficient is no longer proportional to the frequency squared throughout the spectrum, as

assumed by the nondispersive models. Thus, the spectral components generated in sea water by a parametric sonar operating within this 'resonant' relaxation frequency range will be subject to entirely different rates of absorption depending on where the mean primary wave frequency is centered; a process which may enhance or degrade the conversion efficiency relative to its potential value in fresh water.

Obviously these remarks do not apply significantly to unsaturated parametric sonars operating at pre-primary wave shock levels in sea water, nor do they apply to high power parametric sonars in sea water whose primary wave frequencies are such that their fourth or fifth self-generated harmonics do not excede 100 kHz. Likewise, high power parametric sonars operating above 1 MHz in sea water may be unaffected unless the difference-frequency component and its harmonics lie in the 'resonant' relaxation frequency range between 100 kHz and 1 MHz.

However, in order to provide effective tests of the saturation limits predicted in this paper, and compare them with previously derived predictions,[1-5] saturated parametric experiments in nondispersive fluids, such as fresh water, are required. Likewise, in order to predict the saturation limit of parametric sonars operating in sea water whose spectrum falls significantly within the 'resonant' relaxation frequency range, it will be necessary to include the effect of 'relaxation absorption', wherever possible, in the nondispersive analytical models.

ACKNOWLEDGMENTS

The author wishes to thank Mr. J. W. Kesner for programming the model derived in this paper and Mr. A. Nelkin, Manager Sonic Technology, Westinghouse R&D Center, for his kind support and encouragement.

APPENDIX A

If the primary wave amplitudes of a parametric source are significantly lower than their respective shock thresholds, the time waveform will be relatively undistorted. Under these conditions it is possible to solve Eq. 2 by means of the method of successive approximation. Basically, this method consists in solving the linear part of the equation by neglecting the nonlinear term to obtain the "first approximation," which is the undistorted time waveform. Substituting this solution in the nonlinear term and integrating the resulting inhomogeneous equation thus gives the "second approximation." The process can then be repeated to obtain higher approximations.

In order to simplify the procedure of selecting the nonlinearly generated spectral components of interest it is convenient to take the Fourier transform of Eq. 2 so that it becomes.

$$\frac{d\hat{P}_\omega}{d\zeta} + (\omega^2/\Lambda)\hat{P}_\omega = \frac{1}{2}\frac{d}{dt} F_\omega\{P^2\} \tag{A-1}$$

where $$F_\omega\{P(\zeta,t')\} = \hat{P}_\omega(\zeta) = \int_{-\infty}^{\infty} P(\zeta,t')e^{-j\omega t'}\, dt' \tag{A-2}$$

and $$F_\omega^{-1}\{P(\zeta)\} = P(\zeta,t') = \frac{1}{2\pi}\int_{-\infty}^{\infty} \hat{P}_\omega(\zeta)e^{j\omega t'}\, d\omega. \tag{A-3}$$

Solving the linear part of Eq. A-1 for a dual frequency parametric source operating simultaneously at angular frequencies ω_1 and ω_2 with peak amplitudes P_{o1} and P_{o2} respectively, and using Eq. A-3, gives the undistorted time waveform,

$$P(\zeta,t') = P_{o1}e^{-\omega_1^2\int_o^\zeta(1/\Lambda)d\zeta}\sin(\omega_1 t') + P_{o2}e^{-\omega_2^2\int_o^\zeta(1/\Lambda)d\zeta}\sin(\omega_2 t') \qquad (A\text{-}4)$$

$$\text{Thus} \quad \frac{d}{dt}F_{\omega_-}\{P^2\} = -\omega_- P_{o1}P_{o2}e^{-(\omega_1^2+\omega_2^2)\int_o^\zeta(1/\Lambda)d\zeta}; \quad \omega_- = (\omega_1 - \omega_2) \qquad (A\text{-}5)$$

where the operator F_{ω_-} selects the difference-frequency component.

Substituting Eq. A-5 in Eq. A-1 thus gives,

$$\frac{dP_{\omega_-}}{d\zeta} + (\omega^2/\Lambda)\tilde{P}_{\omega_-} = -(\omega_-/2)P_{o1}P_{o2}e^{-(\omega_1^2+\omega_2^2)\int_o^\zeta(1/\Lambda)d\zeta}. \qquad (A\text{-}6)$$

Assuming that the source does not radiate directly at the difference-frequency, then $P_{\omega_-}(o) = 0$. The solution of Eq. A-6 which is the "second approximation" can thus be expressed as,

$$\tilde{P}_{\omega_-}(\zeta) = -(\omega_-/2)P_{o1}P_{o2}e^{-\omega_-^2\int_o^\zeta(1/\Lambda)d\zeta}\int_o^\zeta e^{-(\omega_1^2+\omega_2^2-\omega_-^2)\int_o^{\zeta'}(1/\Lambda)d\zeta''}d\zeta' \qquad (A\text{-}7)$$

For the case of infinity plane waves ($\ell = 0$) Table II gives,

$$\zeta = \sigma_o'(r/r_o), \text{ so that } d\zeta = \sigma_o'(dr/r_o) \qquad (A\text{-}8)$$

and

$$\int_o^\zeta(1/\Lambda)d\zeta = \zeta/\Lambda_o = r\delta. \qquad (A\text{-}9)$$

Substituting Eqs. A-8 and A-9 in Eq. A-7, with $\tilde{P}_{\omega_-} = p_-'/p_o$, it becomes,

$$p_-'(r)/p_o = -(\omega_-/\omega_o)(\sigma_o/2)(P_{o1}P_{o2})e^{-\alpha_- r}\int_o^r e^{-\alpha_T r'}\frac{dr'}{r_o}$$

$$= -(\omega_-/\omega_o)(\sigma_{1,2}/2)e^{-\alpha_- r}\int_o^r e^{-\alpha_T r'}\frac{dr'}{r_o} \qquad (A\text{-}10)$$

where $\sigma_o = \sigma_o'\omega_o$, and $\sigma_{1,2} = \sigma_o P_{o1}P_{o2} = \sigma_o(p_{o1}p_{o2}/p_o^2)$ (A-11)

with $\alpha_i = \delta\omega_i^2$, $\alpha_- = \delta\omega_-^2$, $\alpha_T = (\alpha_1 + \alpha_2 - \alpha_-)$; $(i = 1,2)$. (A-12)

It should be noted that Eq. A-10 is the approximate solution originally obtained by Naugol'nykh, Soluyan and Khokhlov.[27]

Likewise, for spherical waves ($\ell = 1$) Table II gives,

$$\zeta = \sigma_o' \ln(r/r_o), \text{ so that } d\zeta = \sigma_o'(dr/r) \tag{A-13}$$

and

$$\int_o^{\zeta} (1/\Lambda)d = (\sigma_o'/\Lambda_o)(e^{\zeta/\sigma_o'} - 1) = (\sigma_o'/\Lambda_o)\left(\frac{r-r_o}{r_o}\right) = (r - r_o)\delta. \tag{A-14}$$

Substituting Eqs. A-13 and A-14 in Eq. A-7, and recalling that the difinition of $\tilde{P}_{\omega_-}$ for $\ell = 1$, given in the list of symbols, is $P_{\omega_-} = (r/r_o)(p_-/p_o)$ gives,

$$p_-'(r)/p_o = -(\omega_-/\omega_o)(\sigma_{1,2}/2)\left\{\int_{r_o}^{r} e^{-\alpha_T(r'-r_o)} \frac{dr'}{r'} (r_o/r)e^{-\alpha_-(r-r_o)}\right\} \tag{A-16}$$

$$= -(\omega_-/\omega_o)(\sigma_{1,2}/2)\{E_1(\alpha_T r_o) - E_1(\alpha_T r)\}\exp(\alpha_T r_o)(r_o/r)e^{-\alpha_- r - r_o)} \tag{A-17}$$

$$\simeq -(\omega_-/\omega_o)(\sigma_{1,2}/2)\{E_1(\alpha_T r_o) - E_1(\alpha_T r)\}(r_o/r)e^{-\alpha_- r}, \quad \alpha_T r_o << 1, \tag{A-18}$$

where Eq. A-18 is the approximate solution derived by Cary[8] and the author.[8,9] The asymptotic far-field forms of Eq. A-18 thus becomes,

$$p_-(r)/p_o = -(\omega_-/\omega_o)(\sigma_{1,2}/2)E_1(\alpha_T r_o)(r_o/r)e^{-\alpha_- r}, \quad \alpha_T r_o << 1, \ \alpha_T r >> 1. \tag{A-19}$$

APPENDIX B

In order to determine the parameters χ_1, χ_2 and n so that Eq. 29 will approach Eqs. 27 and 28 for the asymptotic extremes of $\alpha_T r_o$ greater and less than unity, respectively, it is expedient to begin with the form of Eq. 29 for small values of χ_i which is,

$$|p'_-(r)p_o| = (\omega_-/\omega_o)^n\{\frac{\chi_1\chi_2}{2\chi_o}\}(r_o/r)e^{-\alpha_- r}, \quad \chi_i << 1, \ (i = 1,2). \tag{B-1}$$

Likewise, for small values of χ'_i (as defined by Eq. 21), Eq. 27 can be expressed as,

$$|p'_-(r)/p_o| \simeq (\omega_-/\omega_o)^2\{(\sigma_{1,2}/2)\int_o^{r_o} e^{-\alpha_T r'}\frac{dr'}{r_o}\}(r_o/r)e^{-\alpha_- r}, \quad \alpha_T r_o >> 1 \tag{B-2}$$

$$\rightarrow (\omega_-/\omega_o)^2(\sigma_{1,2}/2\alpha_T r_o)(r_o/r)e^{-\alpha_- r}.$$

Again, for small values of χ''_i (as defined by Eq. 25), Eq. 28 can be expressed as,

$$|p'_-(r)/p_o| \simeq (\omega_-/\omega_o)\{(\sigma_{1,2}/2)\int_{r_o}^{\infty} e^{-\alpha_T r'}\frac{dr'}{r'}\}(r_o/r)e^{-\alpha_- r}, \quad \alpha_T r_o << 1 \tag{B-3}$$

$$\rightarrow (\omega_-/\omega_o)(\sigma_{1,2}/2)E_1(\alpha_T r_o)(r_o/r)e^{-\alpha_- r}.$$

Combining Eqs. B2 and B3 thus gives,

$$|p'_-(r)/p_o| \simeq (\omega_-/\omega_o)(\sigma_{1,2}/2)\{(\omega_-/\omega_o)\int_o^{r_o} e^{-\alpha_T r'}\frac{dr'}{r_o} + \int_{r_o}^{\infty} e^{-\alpha_T r'}\frac{dr'}{r'}\}(r_o/r)e^{-\alpha_- r}$$

$$\approx (\omega_-/\omega_o)(\sigma_{1,2}/2)\{\int_{r_o}^{\infty}\frac{e^{-\alpha_T r'}}{r'_o + r'}dr'\}(r_o/r)e^{-\alpha_- r}; \ r'_o = r_o(\omega_o/\omega_-)$$

$$= (\omega_-/\omega_o)(\sigma_{1,2}/2)\{E_1(\alpha_T r'_o)\exp(\alpha_T r'_o)\}(r_o/r)e^{-\alpha_- r}. \tag{B-4}$$

Equation B-4 which was previously derived by the author[3] as shown in Table Ia can be reexpressed in terms of $\alpha_T r_o$ as follows:

$$|p'_-(r)/p_o| = (\omega_-/\omega_o)^n(\sigma_{1,2})\{E_1(\alpha_T r_o)\exp(\alpha_T r_o)\}(r_o/r)e^{-\alpha_- r} \qquad \text{(B-5)}$$

where the index n is obtained by equating Eqs. B-4 and B-5 to give,

$$n = 1 + \{\frac{\log_{10}(\Delta/\Delta')}{\log_{10}(\omega_o/\omega_-)}\} \qquad \text{(B-6)}$$

with $\Delta = E_1(\alpha_T r_o)\exp(\alpha_T r_o)$ and $\Delta' = E_1(\alpha_T r'_o)\exp(\alpha_T r'_o)$. (B-7)

Equating Eqs. B-1 and B-5 thus gives χ_i and χ_o as,

$$\chi_i = \sigma_i\Delta \text{ and } \chi_o = \sigma_o\Delta. \qquad \text{(B-8)}$$

REFERENCES

1. R. H. Mellen and M. B. Moffett, "A Model for Parametric Sonar Radiator Design," Naval Underwater Systems Center Tech. Memorandum No. PA41-229-71 (1971).
2. R. H. Mellen and M. B. Moffett, "An Approximate Model for Parametric Acoustic Source Design," 83rd Meeting of the Acoustical Society of America, Buffalo, New York (April 1972), Paper F7.
3. F. H. Fenlon, "On the Performance of a Dual Frequency Parametric Source via Matched Asymptotic Solutions of Burgers' Equation," J. Acoust. Soc. Am. 55, 35-46 (1974).
4. H. O. Berktay and D. J. Leahy, "Farfield Performance of Parametric Transmitters," J. Acoust. Soc. Am. 55, 539-546 (1974).
5. J. F. Bartram, "A Useful Analytical Model for the Parametric Acoustic Array," J. Acoust. Soc. Am., 52, 1042-1044 (1972).
6. D. T. Blackstock, "Approximate Equations Governing Finite-Amplitude Sound in Thermo Viscous Fluids," Suppl. Tech. Rept. AFOSR-5223 (AD415 442) (May 1963).
7. P. J. Westervelt, "Parametric Acoustic Array," J. Acoust. Soc. Am. 35, 535-537 (1963).
8. B. B. Cary and F. H. Fenlon, "On the Exploitation of Parametric Effects in Acoustic Arrays," General Dynamics Report GDED 67-28, 1967.

9. F. H. Fenlon, "A Recursive Procedure for Computing the Nonlinear Spectral Interactions of Progressive Finite-Amplitude Waves in Nondispersive Fluids," J. Acoust. Soc. Am. 50, 1299-1312 (1971).

10. S. J. Tjotta, "Some Nonlinear Effects in Sound Fields," J. Sound Vib. 6, 255-267 (1967).

11. H. Hobaek and M. Vestrheim, "Axial Distribution of Difference-Frequency Sound in a Collimated Beam of Circular Cross Section," Proc. Symp. Nonlinear Acoust., University of Birmingham (England) (April 1971), pp. 137-158.

12. D. T. Blackstock (personal communication).

13. F. H. Fenlon, "An Extension of the Bessel-Fubini Series for a Multiple-Frequency CW Acoustic Source of Finite-Amplitude," J. Acoust. Soc. Am. 51, 284-289 (1972).

14. H. M. Merklinger, R. H. Mellen, and M. B. Moffett, "Finite-Amplitude Losses in Spherical Sound Waves," 84th Meeting of the Acoustical Society of America, Miami, Florida (Dec. 1972), Paper VV9.

15. H. T. Davis, "Introduction to Nonlinear Differential and Integral Equations," (Dover Publications Inc., New York 1962), p. 58.

16. H. M. Merklinger, "High Intensity Effects in the Nonlinear Acoustic End-Fire Array," Ph.D. Thesis, University of Birmingham (England) (June 1971), pp. 145-152.

17. H. M. Merklinger, "Fundamental-Frequency Component of a Finite-Amplitude Plane Wave," J. Acoust. Soc. Am. 54, 1760-1761 (L) (1973).

18. P. J. Westervelt, "Self-Scattering of High Intensity Sound," Proc. 3rd Int. Cong. on Acoustics Stuttgart (Elsevier Publishing Co. Amsterdam 1961), pp. 316-321.

19. S. Wiener, "Standing Sound Waves of Finite Amplitude," J. Acoust. Soc. Am. 40, 240-243 (1966).

20. J. A. Shooter, T. G. Muir, and D. T. Blackstock, "Acoustic Saturation of Spherical Waves in Water," J. Acoust. Soc. Am. 55, 54-62 (1974).

21. B. B. Cary (personal communication).

22. D. T. Blackstock, "On Plane, Spherical, and Cylindrical Sound Waves of Finite Amplitude in Lossless Fluids," J. Acoust. Soc. Am. 36, 217-219 (L) (1964).

23. E. Hopf, "The Partial Differential Equation $u_t + uu_x = \mu u_{xx}$," Comm. Pure Appl. Math. 3, 201-230 (1950).

24. J. D. Cole, "On a Quasi-Linear Parabolic Equation Occurring in Aerodynamics," Quart. Jnl. Appl. Math. 9, 225-236 (1951).

25. P. M. Morse and H. Feshbach, "Methods of Theoretical Physics," (McGraw-Hill, New York 1953), pp. 1322-1323.

26. G. Goertzel and N. Tralli, "Some Mathematical Methods of Physics" (McGraw-Hill, New York 1960), p. 113.

27. K. A. Naugol'nykh, S. I. Soluyan, and R. V. Khokhlov, "Nonlinear Interaction of Sound Waves in an Absorbing Medium," Sov. Phys. Acoust. 9, 155-159 (1963).

28. T. G. Muir, "An Analysis of the Parametric Acoustic Array for Spherical Wave Fields," Ph.D. Thesis, the University of Texas, Austin, Texas (May 1971).

29. J. E. Blue, "Nonlinear Acoustics in Undersea Communication," J.U.A. 22, 177-187 (1972).

30. J. C. Lockwood, "Two Problems in High-Intensity Sound," Ph.D. Thesis The University of Rochester, New York (July 1971).

31. J. C. Lockwood, T. G. Muir, and D. T. Blackstock, "Directive Harmonic Generation in the Radiation Field of a Circular Piston," J. Acoust. Soc. Am. 53, 1148-1153 (1973).

32. H. M. Merklinger, Ibid. 15, pp. 109-112.

33. D. R. Childs, "Beam Patterns and Directivity Indices of Parametric Acoustic Arrays," Proc. Symp. Finite-Amplitude Wave Effects in Fluids, Technical University of Denmark, Copenhagen (August 1973).

34. R. H. Mellen, W. Konrad, and D. G. Browning, "Approximate Sclaing Laws for Parametric Sonar Transmitter Design," Ibid. II, pp. 184-196.

35. W. L. Konrad, R. H. Mellen, and J. L. Nelson, "Farfield Interactions in the Parametric Radiator," Ibid. 2, Paper F8.

36. W. L. Konrad, "Application of the Parametric Source to Bottom and Subbottom Profiling," Ibid. 33.

37. T. G. Muir and J. G. Willette, "Parametric Acoustic Transmitting Arrays," J. Acoust. Soc. Am. 52, 1481-1486 (1972).

38. A. I. Eller, "Adaptation of the NRL Acoustic Tank Facility for Experiments in Parametric Sonar with Preliminary Results," NRL Report 7513 (January 1973).

39. M. Schulkin and H. W. Marsh, "Absorption and Sound in Sea Water," J. Brit. IRE, 25, 493 (1963).